.

QUANTUM FOAM, GRAVITY

AND

GRAVITATIONAL WAVES

Reginald T. Cahill

School of Chemistry, Physics and Earth Sciences

Flinders University

GPO Box 2100, Adelaide 5001, Australia

Reg.Cahill@flinders.edu.au

Process Physics URL:
http://www.scieng.flinders.edu.au/cpes/people/cahill_r/processphysics.html

- September 2003 -

Abstract

It is shown that both the Newtonian and General Relativity theories for gravity may be re-formulated as in-flow dynamics in which a substratum is effectively absorbed by matter, with the gravitational force determined by inhomogeneities of that flow. Analysis herein of the 1925-26 Dayton Miller interferometer data reveals such a gravitational in-flow of space past the Earth into the Sun. This data and that from the 1991 Roland DeWitte coaxial cable experiment also suggests that the in-flow is turbulent, which amounts to the observation of a gravitational wave phenomena. A generalisation of the in-flow formalisms is proposed which passes all the tests that General Relativity passed, but as well the new theory suggests that the so-called spiral galaxy rotation-velocity anomaly may be explained without the need of 'dark matter'. As well analysis of data from the Michelson and Morley, Miller, Illingworth, Jaseja *et al*, Torr and Kolen, and DeWitte experiments reveal motion relative to the substratum. Special relativity effects are caused by motion relative to the substratum. This implies that a new ontology underlies the spacetime formalism.

Contents

1   Introduction

The new information-theoretic *Process Physics* [1, 2, 3, 4, 5, 6] provides for the first time an explanation of space as a decohering quantum foam system in which gravity is an inhomogeneous flow of the quantum foam into matter. As shown herein analysis of data from various Michelson interferometer experiments has demonstrated that absolute motion relative to space had been observed by Michelson and Morley [7], Miller [8], Illingworth [9] and Jaseja *et al* [10] contrary to common belief within physics that absolute motion has never been observed. The key discovery being that the presence of a gas is required in order that a Michelson interferometer [11] be able to detect motion relative to the quantum-foam substratum of space. This effect has gone unnoticed for over

100 years. All gas-mode Michelson interferometers have detected absolute motion but, because the role of the gas had not been realised, the analysis of the data had been incorrect, except for the experiment by Miller who cleverly developed a technique to bypass the long-term deficiency in understanding of the interferometer. Vacuum operated Michelson interferometers are 'blind' to absolute motion. This has also gone unnoticed and has resulted in enormous confusion in the understanding of the experimental study of relativistic effects. Here a comprehensive analysis of the above data is presented together with the data from the non-interferometer experiments by Torr and Kolen [12], and by DeWitte [13]. All these experiments agree on the direction and speed of absolute motion of the solar system through the quantum-foam substratum.

The Dayton Miller extensive Michelson interferometer experimental data also reveals, as shown here, the in-flow of space into the Sun which manifests as gravity, as well as the orbital motion of the Earth about the Sun. The experimental data suggests that the in-flow is turbulent, which amounts to the observation of a gravitational wave phenomena. The DeWitte data also indicates a similar level of turbulence in the in-flow.

The extensive experimental data shows that absolute motion is consistent with relativistic effects. Indeed relativistic effects are caused by dynamical effects associated with absolute motion, as proposed by Lorentz. The Lorentz transformation is seen to be a consequence of absolute motion dynamics. Vacuum Michelson interferometer experiments or its equivalent [14, 15, 16, 17, 18] cannot detect absolute motion, but their null results do support this interpretation and form a part of the experimental predictions of the new physics.

A new in-flow theory of gravity in the classical limit is proposed. It passes all the standard tests that the Newtonian and the General Relativity theories of gravity have passed, including the operation of the Global Positioning System. However it appears that this new theory may explain as well the spiral galaxy rotation-velocity anomaly without invoking dark matter. As well this new theory is expected to predict the turbulent flow which is manifested in the existing experimental observations of absolute motion. Other gravitational anomalies also now appear to be capable of being explained. These developments amount to new physics.

This paper has two main sections, **2.In-Flow as Gravity** which presents the origin and properties of this new theory of gravity, and **3.Observations of Absolute Motion and In-Flow** which analyses the extensive data that supports this new theory of gravity. Significantly this new theory departs from both the Newtonian and General Relativity theories in key aspects, and these experimental signatures are evident in the experimental data. This new theory of gravity has stimulated new experiments to study in particular the new gravitational wave phenomena. Because of the significant development of our understanding of how to detect absolute motion and *ipso facto* gravitational in-flows these new experiments are basically bench-top experiments. One such experiment is operating at Flinders university under the direction of Professor Warren Lawrance, and a report of the analysis of the data will be soon forthcoming.

2 In-Flow as Gravity

2.1 Newtonian Inflow

We begin here the analysis that will lead to the new theory and explanation of gravity. In this theory gravitational effects are caused solely by an inhomogeneous flow of the quantum foam. This is not a flow through space, but essentially a rearrangement of the quantum-foam which globally is most easily described as a flow. This is a subtle aspect of this new physics. The new information-theoretic concepts underlying this physics were discussed in [1, 2]. Essentially matter effectively acts as a 'sink' for that quantum foam. To begin with it should be noted that even Newtonian gravity is suggestive of a flow explanation of gravity. In that theory the gravitational acceleration $\mathbf{g}$ is determined by the matter density ρ according to

$$\nabla.\mathbf{g} = -4\pi G\rho. \tag{1}$$

For $\nabla \times \mathbf{g} = 0$ this gravitational acceleration $\mathbf{g}$ may be written as the gradient of the gravitational potential Φ,

$$\mathbf{g} = -\nabla\Phi, \tag{2}$$

where the gravitational potential is now determined by $\nabla^2\Phi = 4\pi G\rho$. Here, as usual, G is the gravitational constant. Now as $\rho \geq 0$ we can choose to have $\Phi \leq 0$ everywhere if $\Phi \to 0$ at infinity. So we can introduce $\mathbf{v}^2 = -2\Phi \geq 0$ where $\mathbf{v}$ is some velocity vector field. Here the value of $\mathbf{v}^2$ is specified, but not the direction of $\mathbf{v}$. Then

$$\mathbf{g} = \frac{1}{2}\nabla(\mathbf{v}^2) = (\mathbf{v}.\nabla)\mathbf{v} + \mathbf{v} \times (\nabla \times \mathbf{v}). \tag{3}$$

For irrotational flow $\nabla \times \mathbf{v} = \mathbf{0}$. Then $\mathbf{g}$ is the usual Euler expression for the acceleration of a fluid element in a time-independent or stationary fluid flow. If the flow is time dependent the Euler expression suggests the extra time-dependent term in

$$\mathbf{g} = (\mathbf{v}.\nabla)\mathbf{v} + \mathbf{v} \times (\nabla \times \mathbf{v}) + \frac{\partial\mathbf{v}}{\partial t}. \tag{4}$$

This equation is then to be accompanied by the 'Newtonian equation' for the flow field

$$\frac{1}{2}\nabla^2(\mathbf{v}^2) = -4\pi G\rho. \tag{5}$$

While this hints at a fluid flow interpretation of Newtonian gravity the fact that the direction of $\mathbf{v}$ is not specified by (5) suggests that some generalisation is to be expected in which the direction of $\mathbf{v}$ is specified. Of course within the fluid flow interpretation (4) and (5) are together equivalent to the Universal Inverse Square Law for Gravity. Indeed for a spherically symmetric distribution of matter of total mass M the velocity field outside of the matter

$$\mathbf{v}(\mathbf{r}) = -\sqrt{\frac{2GM}{r}}\,\hat{\mathbf{r}}, \tag{6}$$

satisfies (5) and reproduces the inverse square law form for **g** using (4):

$$\mathbf{g} = -\frac{GM}{r^2}\hat{\mathbf{r}}. \tag{7}$$

The in-flow direction $-\hat{\mathbf{r}}$ in (6) may be replaced by any other direction, in which case however the direction of **g** in (7) remains radial.

Of the many new effects predicted by the generalisation of (5), see section 2.7, one is that this 'Inverse Square Law' is only valid outside of spherically symmetric matter systems. Then, for example, the 'Inverse Square Law' is expected to be inapplicable to spiral galaxies. The incorrect assumption of the universal validity of this law led to the notion of 'dark matter' in order to reconcile the faster observed rotation velocities of matter within such galaxies compared to that predicted by the above law.

2.2   Quantum Foam In-Flow

To arrive at the new in-flow theory of gravity we require that the velocity field $\mathbf{v}(\mathbf{r}, t)$ be specified and measurable with respect to a suitable frame of reference. We shall use the Cosmic Microwave Background (CMB) frame of reference for that purpose [19]; see also section 3.9. Then an 'object' has velocity $\mathbf{v}_0(t) = d\mathbf{r}_0(t)/dt$ with respect to that CMB frame, where $\mathbf{r}_0(t)$ is the position of the object wrt that frame. We then define

$$\mathbf{v}_R(t) = \mathbf{v}_0(t) - \mathbf{v}(\mathbf{r}_0(t), t), \tag{8}$$

as the velocity of the object relative to the quantum foam at the location of the object.

Process Physics leads to the Lorentzian interpretation of so called 'relativistic effects'. This means that the speed of light is only 'c' wrt the quantum-foam system, and that time dilation effects for clocks and length contraction effects for rods are caused by the motion of clocks and rods relative to the quantum foam. So these effects are real dynamical effects caused by the quantum foam. We conjecture that the path of an object through an inhomogeneous and time-varying quantum-foam is determined by a variational principle, namely the path $\mathbf{r}_0(t)$ minimises the travel time (for early investigations of the in-flow approach to gravity see Ives [20] and Kirkwood [21, 22]),

$$\tau[\mathbf{r}_0] = \int dt \left(1 - \frac{\mathbf{v}_R^2}{c^2}\right)^{1/2}, \tag{9}$$

with $\mathbf{v}_R$ given by (8). Under a deformation of the trajectory $\mathbf{r}_0(t) \rightarrow \mathbf{r}_0(t) + \delta\mathbf{r}_0(t)$, $\mathbf{v}_0(t) \rightarrow \mathbf{v}_0(t) + \dfrac{d\delta\mathbf{r}_0(t)}{dt}$, and we also have

$$\mathbf{v}(\mathbf{r}_0(t) + \delta\mathbf{r}_0(t), t) = \mathbf{v}(\mathbf{r}_0(t), t) + (\delta\mathbf{r}_0(t).\nabla)\mathbf{v}(\mathbf{r}_0(t)) + ... \tag{10}$$

Then

$$\delta\tau = \tau[\mathbf{r}_0 + \delta\mathbf{r}_0] - \tau[\mathbf{r}_0]$$

$$= -\int dt \, \frac{1}{c^2} \mathbf{v}_R . \delta \mathbf{v}_R \left(1 - \frac{\mathbf{v}_R^2}{c^2} \right)^{-1/2} + ...$$

$$= \int dt \frac{1}{c^2} \left(\mathbf{v}_R . (\delta \mathbf{r}_0 . \nabla) \mathbf{v} - \mathbf{v}_R . \frac{d(\delta \mathbf{r}_0)}{dt} \right) \left(1 - \frac{\mathbf{v}_R^2}{c^2} \right)^{-1/2} + ...$$

$$= \int dt \frac{1}{c^2} \left(\frac{\mathbf{v}_R . (\delta \mathbf{r}_0 . \nabla) \mathbf{v}}{\sqrt{1 - \frac{\mathbf{v}_R^2}{c^2}}} + \delta \mathbf{r}_0 . \frac{d}{dt} \frac{\mathbf{v}_R}{\sqrt{1 - \frac{\mathbf{v}_R^2}{c^2}}} \right) + ...$$

$$= \int dt \, \frac{1}{c^2} \delta \mathbf{r}_0 . \left(\frac{(\mathbf{v}_R . \nabla) \mathbf{v} + \mathbf{v}_R \times (\nabla \times \mathbf{v})}{\sqrt{1 - \frac{\mathbf{v}_R^2}{c^2}}} + \frac{d}{dt} \frac{\mathbf{v}_R}{\sqrt{1 - \frac{\mathbf{v}_R^2}{c^2}}} \right) + ... \tag{11}$$

Hence a trajectory $\mathbf{r}_0(t)$ determined by $\delta\tau = 0$ to $O(\delta\mathbf{r}_0(t)^2)$ satisfies

$$\frac{d}{dt} \frac{\mathbf{v}_R}{\sqrt{1 - \frac{\mathbf{v}_R^2}{c^2}}} = - \frac{(\mathbf{v}_R . \nabla) \mathbf{v} + \mathbf{v}_R \times (\nabla \times \mathbf{v})}{\sqrt{1 - \frac{\mathbf{v}_R^2}{c^2}}}. \tag{12}$$

Let us now write this in a more explicit form. This will also allow the low speed limit to be identified. Substituting $\mathbf{v}_R(t) = \mathbf{v}_0(t) - \mathbf{v}(\mathbf{r}_0(t), t)$ and using

$$\frac{d\mathbf{v}(\mathbf{r}_0(t), t)}{dt} = (\mathbf{v}_0 . \nabla) \mathbf{v} + \frac{\partial \mathbf{v}}{\partial t}, \tag{13}$$

we obtain

$$\frac{d}{dt} \frac{\mathbf{v}_0}{\sqrt{1 - \frac{\mathbf{v}_R^2}{c^2}}} = \mathbf{v} \frac{d}{dt} \frac{1}{\sqrt{1 - \frac{\mathbf{v}_R^2}{c^2}}} + \frac{(\mathbf{v} . \nabla) \mathbf{v} - \mathbf{v}_R \times (\nabla \times \mathbf{v}) + \frac{\partial \mathbf{v}}{\partial t}}{\sqrt{1 - \frac{\mathbf{v}_R^2}{c^2}}}. \tag{14}$$

Then in the low speed limit $v_R \ll c$ we obtain

$$\frac{d\mathbf{v}_0}{dt} = (\mathbf{v} . \nabla) \mathbf{v} - \mathbf{v}_R \times (\nabla \times \mathbf{v}) + \frac{\partial \mathbf{v}}{\partial t} = \mathbf{g}(\mathbf{r}_0(t), t) + (\nabla \times \mathbf{v}) \times \mathbf{v}_0, \tag{15}$$

which agrees with the 'Newtonian' form (4) for zero vorticity ($\nabla \times \mathbf{v} = 0$). Hence (14) is a generalisation of (4) to include Lorentzian dynamical effects, for in (14) we can multiply both sides by the rest mass m_0 of the object, and then (14) involves

$$m(\mathbf{v}_R) = \frac{m_0}{\sqrt{1 - \frac{\mathbf{v}_R^2}{c^2}}}, \tag{16}$$

the so called 'relativistic' mass, and (14) acquires the form

$$\frac{d}{dt}(m(\mathbf{v}_R)\mathbf{v}_0) = \mathbf{F},\tag{17}$$

where $\mathbf{F}$ is an effective 'force' caused by the inhomogeneities and time-variation of the flow. This is essentially Newton's 2nd Law of Motion in the case of gravity only. That m_0 cancels is the equivalence principle, and which acquires a simple explanation in terms of the flow. Note that the occurrence of $1/\sqrt{1 - \frac{\mathbf{v}_R^2}{c^2}}$ will lead to the precession of the perihelion of planetary orbits, and also to horizon effects wherever $|\mathbf{v}| = c$: the region where $|\mathbf{v}| < c$ is inaccessible from the region where $|\mathbf{v}| > c$. Also (9), in conjunction with (51), is easily used to show that the new theory of gravity agrees with that of General Relativity for the operation of the GPS satellite navigation system, when the in-flow is given by (6); see section 2.10.

Equation (9) involves various absolute quantities such as the absolute velocity of an object relative to the quantum foam and the absolute speed c also relative to the foam, and of course absolute velocities are excluded from the General Relativity (GR) formalism. However (9) gives (with $t \equiv x_0^0$)

$$d\tau^2 = dt^2 - \frac{1}{c^2}(d\mathbf{r}_0(t) - \mathbf{v}(\mathbf{r}_0(t), t)dt)^2 = g_{\mu\nu}(x_0)dx_0^\mu dx_0^\nu,\tag{18}$$

which is the Panlevé-Gullstrand [23, 24] form of the metric $g_{\mu\nu}$ for GR. All of the above is very suggestive that useful information for the flow dynamics may be obtained from GR by restricting the choice of metric to the Panlevé-Gullstrand form. We emphasize that the absolute velocity $\mathbf{v}_R$ has been measured, see section 3.4, and so this in-flow theory of gravity is no longer speculative.

2.3   Apparent Invariance of c

The quantum foam induces actual dynamical time dilations and length contractions in agreement with the Lorentz interpretation of special relativistic effects. As a consequence of this observers in uniform motion 'through' the foam will on measurement of the speed of light obtain always the same numerical value c, so long as they do not adjust their observational data to take account of these dynamical effects. So the special relativistic effects are very much an aspect of physical reality, but nevertheless the absolute motion causing these effects is observable.

To see this explicitly consider how various observers $P, P', ..$ moving with different speeds through the foam, might measure the speed of light. They each acquire a standard rod and an accompanying standardised clock. That means that these standard rods would agree if they were brought together, and at rest with respect to the quantum foam they would all have length Δl_0, and similarly for the clocks. Observer P and accompanying rod are both moving at speed v_R relative to the quantum foam, with the rod longitudinal to that motion, for simplicity. P then measures the time Δt_R, with the clock at end A of the rod, for a light pulse to travel from end A to the other end B and back again to A. The light travels at speed c relative to the quantum-foam. Let the

time taken for the light pulse to travel from $A \to B$ be t_{AB} and from $B \to A$ be t_{BA}, as measured by a clock at rest with respect to the quantum foam. The length of the rod moving at speed v_R is contracted to

$$\Delta l_R = \Delta l_0 \sqrt{1 - \frac{v_R^2}{c^2}}. \tag{19}$$

In moving from A to B the light must travel an extra distance because the end B travels a distance $v_R t_{AB}$ in this time, thus the total distance that must be traversed is

$$ct_{AB} = \Delta l_R + v_R t_{AB}, \tag{20}$$

Similarly on returning from B to A the light must travel the distance

$$ct_{BA} = \Delta l_R - v_R t_{BA}. \tag{21}$$

Hence the total travel time Δt_0 is

$$\Delta t_0 = t_{AB} + t_{BA} \quad = \quad \frac{\Delta l_R}{c - v_R} + \frac{\Delta l_R}{c + v_R} \tag{22}$$

$$= \quad \frac{2\Delta l_0}{c\sqrt{1 - \frac{v_R^2}{c^2}}}. \tag{23}$$

Because of the time dilation effect for the moving clock

$$\Delta t_R = \Delta t_0 \sqrt{1 - \frac{v_R^2}{c^2}}. \tag{24}$$

Then for the moving observer the speed of light is defined as the distance the observer believes the light travelled ($2\Delta l_0$) divided by the travel time according to the accompanying clock (Δt_R), namely $2\Delta l_0/\Delta t_R = c$. So the speed v_R of the observer through the quantum foam is not revealed by this procedure, and the observer is erroneously led to the conclusion that the speed of light is always c. This *invariance of c* follows from two or more observers in manifest relative motion all obtaining the same speed c by this procedure. Despite this failure this special effect is actually the basis of the spacetime measurement protocol. That this protocol is blind to the absolute motion has led to enormous confusion within physics. However it is possible to overcome the 'blindness' of this procedure and to manifestly reveal an observer's absolute velocity of motion v_R. A simple way to do this is shown in figure 1. This involves two identical antiparallel lasers. Then the difference in travel time through vacuum to the detector is

$$\Delta t \quad = \quad \frac{L}{c - v_R} - \frac{L}{c + v_R},$$

$$= \quad 2\frac{L}{c}\frac{v_R}{c} + O(\frac{v_R^2}{c^2}). \tag{25}$$

which is a 1st-order effect, and for that reason the time dilation and length contraction effects have been neglected. Here for simplicity v_R is along the axis of the instrument. The speed v_R is determined from the variation in beat frequency as the device is rotated. The main technical difficulty is in maintaining the frequency stability of the two lasers. It is important to note that this device does not require synchronisation of the two clocks (here lasers). If the two arms are placed at 90^0 to each other as in the New Bedford experiment, see section 3.6, then the effect becomes null. To obtain a non-null effect in this arrangement a gas is required in the air-paths. In the New Bedford experiment that gas was in the masers. This is one of many experiments where the role of a gas in an interferometer has played a critical but, until now, unrecognised role.
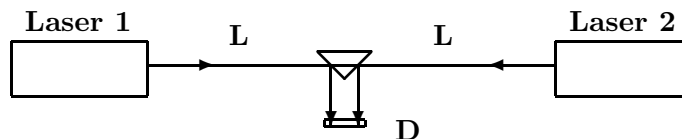

Figure 1: A 1st-order device for detecting absolute motion. Light from two identical lasers is combined and their beat frequency is detected at D.

2.4 The Lorentz Transformation

Here we show that the real dynamical effects of absolute moton results in certain special observational data being related by the Lorentz transformation. This involves the use of the radar measurement protocol for acquiring observational space and time data of distant events, and subsequently displaying that data in a spacetime construct. In this protocol the observer records the time of emission and reception of radar pulses $(t_r > t_e)$ travelling through the space of quantum foam, and then retrospectively assigns the time and distance of a distant event B according to (ignoring directional information for simplicity)

$$T_B = \frac{1}{2}(t_r + t_e), \quad D_B = \frac{c}{2}(t_r - t_e), \tag{26}$$

where each observer is now using the same numerical value of c. The event B is then plotted as a point in an individual geometrical construct by each observer, known as a spacetime record, with coordinates (D_B, T_B). This is no different to a historian recording events according to some agreed protocol. We now show that because of this protocol and the quantum foam dynamical effects, observers will discover on comparing their historical records of the same events that the expression

$$\tau_{AB}^2 = T_{AB}^2 - \frac{1}{c^2}D_{AB}^2, \tag{27}$$

is an invariant, where $T_{AB} = T_A - T_B$ and $D_{AB} = D_A - D_B$ are the differences in times and distances assigned to events A and B using the above measurement protocol (26),

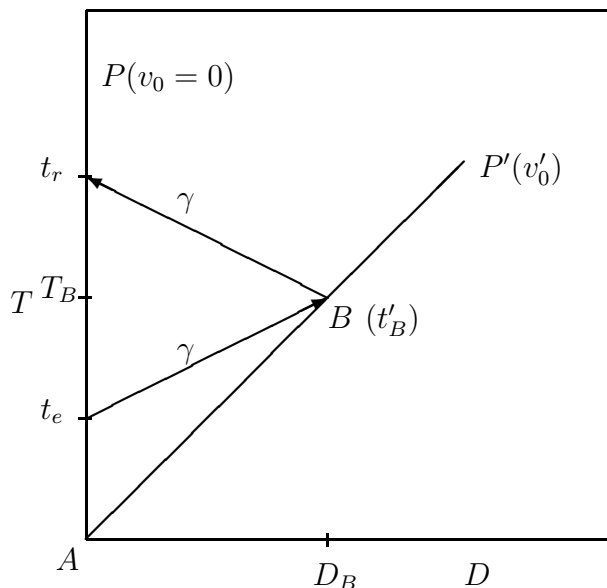so long as both are sufficiently small compared with the scale of inhomogeneities in the velocity field.

Figure 2: Here $T - D$ is the spacetime construct (from the measurement protocol) of a special observer P *at rest* wrt the quantum foam, so that $v_0 = 0$. Observer P' is moving with speed v_0' as determined by observer P, and therefore with speed $v_R' = v_0'$ wrt the quantum foam. Two light pulses are shown, each travelling at speed c wrt both P and the quantum foam. As we see later these one-way speeds for light, relative to the quantum foam, are equal by observation. Event A is when the observers pass, and is also used to define zero time for each for convenience.

To confirm the invariant nature of the construct in (27) one must pay careful attention to observational times as distinct from protocol times and distances, and this must be done separately for each observer. This can be tedious. We now demonstrate this for the situation illustrated in figure2.

By definition the speed of P' according to P is $v_0' = D_B/T_B$ and so $v_R' = v_0'$, where T_B and D_B are the protocol time and distance for event B for observer P according to (26). Then using (27) P would find that $(\tau_{AB}^P)^2 = T_B^2 - \frac{1}{c^2}D_B^2$ since both $T_A = 0$ and $D_A=0$, and whence $(\tau_{AB}^P)^2 = (1 - \frac{v_R'^2}{c^2})T_B^2 = (t_B')^2$ where the last equality follows from the time dilation effect on the P' clock, since t_B' is the time of event B according to that clock. Then T_B is also the time that P' would compute for event B when correcting for the time-dilation effect, as the speed v_R' of P' through the quantum foam is observable by P'. Then T_B is the 'common time' for event B assigned by both observers. For P' we obtain directly, also from (26) and (27), that $(\tau_{AB}^{P'})^2 = (T_B')^2 - \frac{1}{c^2}(D_B')^2 = (t_B')^2$, as $D_B' = 0$ and $T_B' = t_B'$. Whence for this situation

$$(\tau_{AB}^P)^2 = (\tau_{AB}^{P'})^2, \tag{28}$$

and so the construction (27) is an invariant.

While so far we have only established the invariance of the construct (27) when one of the observers is at rest wrt to the quantum foam, it follows that for two observers P' and P'' both in motion wrt the quantum foam it follows that they also agree on the invariance of (27). This is easily seen by using the intermediate step of a stationary observer P:

$$(\tau_{AB}^{P'})^2 = (\tau_{AB}^{P})^2 = (\tau_{AB}^{P''})^2. \tag{29}$$

Hence the protocol and Lorentzian effects result in the construction in (27) being indeed an invariant in general. This is a remarkable and subtle result. For Einstein this invariance was a fundamental assumption, but here it is a derived result, but one which is nevertheless deeply misleading. Explicitly indicating small quantities by Δ prefixes, and on comparing records retrospectively, an ensemble of nearby observers agree on the invariant

$$\Delta\tau^2 = \Delta T^2 - \frac{1}{c^2}\Delta D^2, \tag{30}$$

for any two nearby events. This implies that their individual patches of spacetime records may be mapped one into the other merely by a change of coordinates, and that collectively the spacetime patches of all may be represented by one pseudo-Riemannian manifold, where the choice of coordinates for this manifold is arbitrary, and we finally arrive at the invariant

$$\Delta\tau^2 = g_{\mu\nu}(x)\Delta x^\mu \Delta x^\nu, \tag{31}$$

with $x^\mu = \{T, D_1, D_2, D_3\}$. For flat metrics (31) is invariant under the well known Lorentz transformation,

$$x^\mu = L(\mathbf{v})^\mu{}_\nu x'^\nu, \tag{32}$$

where, for motion only in the x-direction,

$$
\begin{aligned}
x &= \gamma(x' - \beta ct') \\
ct &= \gamma(ct' - \beta x') \\
y &= y' \\
z &= z'
\end{aligned}
\tag{33}
$$

where $\beta = v/c$ and $\gamma = 1/\sqrt{1-\beta^2}$. Here, in general, $\mathbf{v}$ is the relative velocity of the two observers, determined by using the measurement protocol. The special feature of this mapping between the observer's spacetime records is that it does *not* involve the absolute velocity of either observer relative to the quantum-foam substratum - their absolute velocities. This feature was responsible for the first two assumptions in (34). This feature has caused enormous confusion in physics. It erroneously suggests that absolute motion is incompatible with relativistic effects - that the observation of absolute motion must be in conflict with the observation of relativistic effects. For that reason reports of the ongoing detection of absolute motion has been banned in physics for nearly 100 years. However to the contrary absolute motion *and* special relativistic effects are both needed to understand and analyse the extensive experimental data reported in section 3. The key insight is that absolute motion dynamically causes the time dilation and length

contraction effects. Without absolute motion there would be no special relativistic effects. This insight runs counter to nearly 100 years of conventional wisdom within physics.

2.5   The General Relativity Formalism

The general relativity formalism is well known. It was constructed by Hilbert and Einstein by amalgamating the special relativity invariance and, in the low speed limit, the Newtonian theory of gravity. This resulted in the need for the key feature of employing a non-flat spacetime manifold. The three key assumptions were:

> **(1)   The laws of physics have the same form in all**
>   **inertial reference frames.**
>
> **(2)   Light propagates through empty space with a**
>   **speed c independent of the speed of the**
>   **(a) source or (b) observer.**
>
> **(3)   In the limit of low speeds the new formalism**
>   **should agree with Newtonian gravity.**   (34)

The first two assumptions, apart from 2(a) which remains completely valid, have restricted truth in that they refer to the dynamical effects of absolute motion, and how those effects enter into the description of physical phenomena when not correcting for the effects of the absolute motion on the observer's measuring clocks and rods. As we shall see the third assumption is actually the weakest for we shall see that the Newtonian theory of gravity was formulated under very special conditions; namely ones of high spherical symmetry. When that symmetry is not present then Newtonian gravity is flawed. There is abundant experimental evidence to support this claim. Hence the weakest part of the general relativity formalism is actually its link to Newtonian gravity. Nevertheless there is something that is partially correct within the formalism for it has passed a number of key tests, albeit with most tests occuring also in cases of high spherical symmetry, as explained later. And so the flaw in general relativity like that of the Newtonian theory has essentially gone unnoticed. Here we analyse the general relativity formalism in order to discover which aspect of it is actually responsible for its few successes. We shall see that in fact in those cases it may be reformulated as an in-flow formalism.

From the above assumptions the equations which specify the metric tensor $g_{\mu\nu}(x)$ of the spacetime construct may be found to be

$$G_{\mu\nu} \equiv R_{\mu\nu} - \frac{1}{2}Rg_{\mu\nu} = \frac{8\pi G}{c^2}T_{\mu\nu}, \tag{35}$$

where $G_{\mu\nu}$ is known as the Einstein tensor, $T_{\mu\nu}$ is the energy-momentum tensor, $R_{\mu\nu} = R^{\alpha}_{\mu\alpha\nu}$ and $R = g^{\mu\nu}R_{\mu\nu}$ and $g^{\mu\nu}$ is the matrix inverse of $g_{\mu\nu}$. The curvature tensor is

$$R^{\rho}_{\mu\sigma\nu} = \Gamma^{\rho}_{\mu\nu,\sigma} - \Gamma^{\rho}_{\mu\sigma,\nu} + \Gamma^{\rho}_{\alpha\sigma}\Gamma^{\alpha}_{\mu\nu} - \Gamma^{\rho}_{\alpha\nu}\Gamma^{\alpha}_{\mu\sigma}, \tag{36}$$

where $\Gamma^{\alpha}_{\mu\sigma}$ is the affine connection

$$\Gamma^{\alpha}_{\mu\sigma} = \frac{1}{2}g^{\alpha\nu}\left(\frac{\partial g_{\nu\mu}}{\partial x^{\sigma}} + \frac{\partial g_{\nu\sigma}}{\partial x^{\mu}} - \frac{\partial g_{\mu\sigma}}{\partial x^{\nu}}\right). \tag{37}$$

In this formalism the trajectories of test objects are determined by

$$\Gamma^{\lambda}_{\mu\nu}\frac{dx^{\mu}}{d\tau}\frac{dx^{\nu}}{d\tau} + \frac{d^2 x^{\lambda}}{d\tau^2} = 0, \tag{38}$$

which is equivalent to minimising the functional

$$\tau[x] = \int dt \sqrt{g^{\mu\nu}\frac{dx^{\mu}}{dt}\frac{dx^{\nu}}{dt}}, \tag{39}$$

wrt to the path $x[t]$.

For the case of a spherically symmetric mass a solution of (35) for $g_{\mu\nu}$ outside of that mass M is the Schwarzschild metric

$$d\tau^2 = (1 - \frac{2GM}{c^2 r})dt^2 - \frac{1}{c^2}r^2(d\theta^2 + \sin^2(\theta)d\phi^2) - \frac{dr^2}{c^2(1 - \frac{2GM}{c^2 r})}. \tag{40}$$

This solution is the basis of various experimental checks of General Relativity in which the spherically symmetric mass is either the Sun or the Earth. The four tests are: the gravitational redshift, the bending of light, the precession of the perihelion of Mercury, and the time delay of radar signals. To these we should add the operation of the GPS; see section 2.10.

However the solution (40) is in fact completely equivalent to the in-flow interpretation of Newtonian gravity. Making the change of variables $t \to t'$ and $\mathbf{r} \to \mathbf{r'} = \mathbf{r}$ with

$$t' = t + \frac{2}{c}\sqrt{\frac{2GMr}{c^2}} - \frac{4GM}{c^2}\tanh^{-1}\sqrt{\frac{2GM}{c^2 r}}, \tag{41}$$

the Schwarzschild solution (40) takes the form

$$d\tau^2 = dt'^2 - \frac{1}{c^2}(dr' + \sqrt{\frac{2GM}{r'}}dt')^2 - \frac{1}{c^2}r'^2(d\theta'^2 + \sin^2(\theta')d\phi'), \tag{42}$$

which is exactly the Panlevé-Gullstrand form of the metric $g_{\mu\nu}$ [23, 24] in (18) with the velocity field given exactly by the Newtonian form in (6). In which case the trajectory equation (38) of test objects in the Schwarzschild metric is equivalent to solving (14). Thus the minimisation of the τ functional in (39) is equivalent to the minimisation of the τ functional in (9). This choice of coordinates corresponds to a particular frame of reference in which the test object has velocity $\mathbf{v}_R = \mathbf{v} - \mathbf{v}_0$ relative to the in-flow field $\mathbf{v}$.

It is conventional wisdom for practitioners in General Relativity to regard the choice of coordinates or frame of reference to be entirely arbitrary and having no physical significance: no observations should be possible that can detect and measure $\mathbf{v}_R$. This

'wisdom' is based on two beliefs (i) that all attempts to detect $\mathbf{v}_R$, namely the detection of absolute motion, have failed, and that (ii) the existence of absolute motion is incompatible with the many successes of both the Special Theory of Relativity. Both of these beliefs are demonstrably false.

The results in this section suggest, just as for Newtonian gravity, that General Relativity is nothing more than the dynamical equations for a velocity flow field $\mathbf{v}(\mathbf{r}, t)$, atleast in those cases where it has been checked.

2.6 General Relativity In-Flow

Here we extract from General Relativity the in-flow formalism. To do this we must clearly adopt the Panlevé-Gullstrand form of the metric $g_{\mu\nu}$ as that corresponding to the observable quantum foam system, namely to an observationally detected special frame of reference. This form for the metric involves a general velocity field $\mathbf{v}(\mathbf{r}, t)$ where for precision we consider the coordinates $\mathbf{r}, t$ as that of observers at rest with respect to the CMB frame. Note that in this frame $\mathbf{v}(\mathbf{r}, t)$ is not necessarily zero, for mass acts as a sink for the flow. We therefore merely substitute the metric

$$d\tau^2 = g_{\mu\nu}dx^\mu dx^\nu = dt^2 - \frac{1}{c^2}(d\mathbf{r}(t) - \mathbf{v}(\mathbf{r}(t), t)dt)^2, \tag{43}$$

into (35) using (37) and (36). This metric involves the arbitrary time-dependent velocity field $\mathbf{v}(\mathbf{r}, t)$. This is a very tedious computation and the results below were obtained by using the symbolic mathematics capabilities of *Mathematica*. The various components of the Einstein tensor are then

$$
\begin{aligned}
G_{00} &= \sum_{i,j=1,2,3} v_i \mathcal{G}_{ij} v_j - c^2 \sum_{j=1,2,3} \mathcal{G}_{0j} v_j - c^2 \sum_{i=1,2,3} v_i \mathcal{G}_{i0} + c^2 \mathcal{G}_{00}, \\
G_{i0} &= -\sum_{j=1,2,3} \mathcal{G}_{ij} v_j + c^2 \mathcal{G}_{i0}, \quad i = 1, 2, 3. \\
G_{ij} &= \mathcal{G}_{ij}, \quad i, j = 1, 2, 3.
\end{aligned}
\tag{44}
$$

where the $\mathcal{G}_{\mu\nu}$ are given by

$$
\begin{aligned}
\mathcal{G}_{00} &= \frac{1}{2}((trD)^2 - tr(D^2)), \\
\mathcal{G}_{i0} &= \mathcal{G}_{0i} = -\frac{1}{2}(\nabla \times (\nabla \times \mathbf{v}))_i, \quad i = 1, 2, 3. \\
\mathcal{G}_{ij} &= \frac{d}{dt}(D_{ij} - \delta_{ij} trD) + (D_{ij} - \frac{1}{2}\delta_{ij} trD)trD \\
&\quad - \frac{1}{2}\delta_{ij} tr(D^2) - (D\Omega - \Omega D)_{ij}, \quad i, j = 1, 2, 3.
\end{aligned}
\tag{45}
$$

Here

$$D_{ij} = \frac{1}{2}\left(\frac{\partial v_i}{\partial x_j} + \frac{\partial v_j}{\partial x_i}\right) \tag{46}$$

is the symmetric part of the rate of strain tensor $\frac{\partial v_i}{\partial x_j}$, while the antisymmetric part is

$$\Omega_{ij} = \frac{1}{2}(\frac{\partial v_i}{\partial x_j} - \frac{\partial v_j}{\partial x_i}). \tag{47}$$

In vacuum, with $T_{\mu\nu} = 0$, we find from (35) and (44) that $G_{\mu\nu} = 0$ implies that $\mathcal{G}_{\mu\nu} = 0$. It is then easy to check that the in-flow velocity field (6) satisfies these equations. This simply expresses the previous observation that this 'Newtonian in-flow' is completely equivalent to the Schwarzschild metric. That the Scwarzschild metric in (40) is nothing more than the Newtonian inverse square law (7) in disguise appears to be poorly known. We note that the vacuum equations $\mathcal{G}_{\mu\nu} = 0$ do not involve the speed of light; it appears only in (44). It is therefore suggested that (44) amounts to the separation of the measurement protocol, which involves c, from the supposed dynamics of gravity within the General Relativity formalism, and which does not involve c. However the details of the vacuum dynamics in (45) have not actually been tested: All the key tests of General Relativity are now seen to amount to a test *only* of $\delta\tau[x]/\delta x^\mu = 0$, which is the minimisation of (9), when the in-flow field is given by (44), and which is nothing more than Newtonian gravity. Of course Newtonian gravity was itself merely based upon observations within the Solar system, and this may have been too special to have revealed key aspects of gravity. Hence, despite popular opinion, the General Relativity formalism is apparently based upon rather poor evidence.

2.7 Generalised In-Flow - a New Theory of Gravity

Despite the limited insight into gravity which General Relativity is now seen to amount to, here we look for possible generalisations of Newtonian gravity and its in-flow interpretation by examining some of the mathematical structures that have arisen in (45). For the case of zero vorticity $\nabla \times \mathbf{v} = 0$ we have $\Omega_{ij} = 0$ and also that we may write $\mathbf{v} = \nabla u$ where $u(\mathbf{r}, t)$ is a scalar field, and only one equation is required to determine u. To that end we consider the trace of $\mathcal{G}_{ij}$. Note that $tr(D) = \nabla.\mathbf{v}$, and that

$$\frac{d(\nabla.\mathbf{v})}{dt} = (\mathbf{v}.\nabla)(\nabla.\mathbf{v}) + \frac{\partial(\nabla.\mathbf{v})}{\partial t}. \tag{48}$$

Then using the identity

$$(\mathbf{v}.\nabla)(\nabla.\mathbf{v}) = \frac{1}{2}\nabla^2(\mathbf{v}^2) - tr(D^2) - \frac{1}{2}(\nabla \times \mathbf{v})^2 + \mathbf{v}.\nabla \times (\nabla \times \mathbf{v}), \tag{49}$$

and imposing

$$\sum_{i=1,2,3} \mathcal{G}_{ii} = -8\pi G\rho, \tag{50}$$

we obtain

$$\frac{\partial}{\partial t}(\nabla.\mathbf{v}) + \frac{1}{2}\nabla^2(\mathbf{v}^2) + \frac{1}{4}((trD)^2 - tr(D^2)) = -4\pi G\rho. \tag{51}$$

This is seen to be a possible generalisation of the Newtonian equation (5). Note that General Relativity has suggested exactly the time derivative of the form suggested by

the Euler fluid flow acceleration in (4) (see also (52)), and also the new term $C(\mathbf{v}) = \frac{1}{4}((trD)^2 - tr(D^2))$. First note that for the case of the Solar system, with the mass concentrated in one object, namely the Sun, we see that the in-flow field (6) satisfies (51) since in this special case $C(\mathbf{v}) = 0$. As we shall see later the presence of the C term is also well hidden when we consider the Earth's gravitational effects, although there are various known anomalies that indicate that a generalisation of Newtonian gravity is required. Hence (51) in the case of the Solar system is indistinguishable from Newtonian gravity, or the Schwarzschild metric within the General Relativity formalism, so long as we use (9), in being able to determine trajectories of test objects. Hence (51) is automatically in agreement with most of the so-called checks on Newtonian gravity and later General Relativity. Note that (51) does not involve the speed of light c. Nevertheless we have not derived (51)) from the underlying Quantum Homotopic Field Theory which arises from the information-theoretic theory in [1], and indeed it is not a consequence of General Relativity, as the $\mathcal{G}_{00}$ equation of (45) requires that $C(\mathbf{v}) = 0$ in vacuum. Equation (51) at this stage should be regarded as a conjecture which will permit the exploration of possible quantum-foam physics, at the classical level, and also allow comparison with experiment.

As well we should comment on two other tests of General Relativity. One is the observed decay of the orbits of binary pulsars. From (16) with the in-flow (6) it is easily seen that circular orbits are stable. However for elliptical orbits not only is there a precession of the orbit but the orbit is not stable. On dimensional grounds we would expect a decay rate of the magnitude observed for binary pulsars. The other test is the prediction of the cosmological curvature of the universe and associated with the Big Bang. As noted in [1] process physics also predicts a growing non-flat universe. These cosmological aspects are clearly not included in (51), which is only applicable to *local* effects.

However one key aspect of (51) should be noted here, namely that being a non-linear fluid-flow dynamical system we would expect the flow to be turbulent, particularly when the matter is not spherically symmetric or inside even a spherically symmetric distribution of matter, since then the $C(\mathbf{v})$ term is non-zero and it will drive that turbulence. In the following sections we shall see that the experiments that reveal absolute motion also reveal evidence of turbulence.

2.8 The 'Dark Matter' Effect

Because of the $C(\mathbf{v})$ term (51) would predict that the Newtonian inverse square law would not be applicable to systems such as spiral galaxies, because of their highly non-spherical distribution of matter. Of course attempts to retain this law, despite its manifest failure, has led to the spurious introduction of the notion of dark matter within spiral galaxies, and also at larger scales. From

$$\mathbf{g} = \frac{1}{2}\nabla(\mathbf{v}^2) + \frac{\partial \mathbf{v}}{\partial t}, \tag{52}$$

which is (4) for irrotational flow, we see that (51) gives

$$\nabla.\mathbf{g} = -4\pi G\rho - C(\mathbf{v}),\tag{53}$$

and taking running time averages to account for turbulence

$$\nabla.<\mathbf{g}>= -4\pi G\rho- <C(\mathbf{v})>,\tag{54}$$

and writing the extra term as $<C(\mathbf{v})>= 4\pi G\rho_{DM}$ we see that ρ_{DM} would act as an effective matter density, and it is suggested that it is the consequences of this term which have been misinterpreted as 'dark matter'. Here we see that this effect is actually the consequence of quantum foam effects within the new proposed dynamics for gravity, and which becomes apparent particularly in spiral galaxies. Note that (51) is an equation for $\mathbf{v}$, and now involves the direction of $\mathbf{v}$, unlike the special case of Newtonian gravity (5). Because $\nabla \times \mathbf{v} = 0$ we can write (51) in the form

$$\mathbf{v}(\mathbf{r},t) = \frac{1}{4\pi} \int^t dt' \int d^3r'(\mathbf{r} - \mathbf{r}')\frac{\frac{1}{2}\nabla^2(\mathbf{v}^2(\mathbf{r}',t')) + 4\pi G\rho(\mathbf{r}',t') + C(\mathbf{v}(\mathbf{r}',t'))}{|\mathbf{r} - \mathbf{r}'|^3},\tag{55}$$

which allows the determination of the time evolution of $\mathbf{v}$.

The new flow dynamics encompassed in (51) thus accounts for most of the known gravitational phenomena, but will lead to some very clear cut experiments that will distinguish it from the two previous attempts to model gravitation. It turns out that these two attempts were based on some key 'accidents' of history. In the case of the Newtonian modelling of gravity the prime 'accident' was of course the Solar system with its high degree of spherical symmetry. In each case we had test objects, namely the planets, in orbit about the Sun, or we had test object in orbit about the Earth. In the case of the General Relativity modelling the prime 'accident' was the mis-reporting of the Michelson-Morley experiment, and the ongoing belief that the so called 'relativistic effects' are incompatible with absolute motion. We shall consider in detail later some further anomalies that might be appropriately explained by this new modelling of gravity. Of course that the in-flow has been present in various experimental data is also a significant argument for something like (51) to model gravity. Key new experimental techniques will enable the consequences of (51) to be tested. If necessary these experiments will provide insights into possible modifications to (51).

2.9   Gravity and Absolute Motion

We consider here why the existence of absolute motion and as well the presence of the $C(\mathbf{v})$ term appears to have escaped attention in the case of gravitational experiments and observations near the Earth, despite the fact, in the case of the $C(\mathbf{v})$ term, that the presence of the Earth breaks the spherical symmetry of the matter distribution of the Sun.

First note that if we have a matter distribution $\rho(\mathbf{r})$ at rest in the space of quantum foam, and that (51) has solution $\mathbf{v}_0(\mathbf{r},t)$, and then with $\mathbf{g}_0(\mathbf{r},t)$ given by (52), then

when the same matter distribution is uniformly translating at velocity $\mathbf{V}$, that is $\rho(\mathbf{r}) \rightarrow \rho(\mathbf{r} - \mathbf{V}t)$, then a solution to (51) is

$$\mathbf{v}(\mathbf{r}, t) = \mathbf{v}_0(\mathbf{r} - \mathbf{V}t, t) + \mathbf{V}. \tag{56}$$

Note that this is a manifestly time-dependent process and the time derivative in (4) or (14) and (51) plays an essential role. As well the result is nontrivial as (51) is a non-linear equation. The solution (56) follows because (i) the expression for the acceleration $\mathbf{g}(\mathbf{r}, t)$ gives, and this expression occurs in (51),

$$
\begin{aligned}
\mathbf{g}(\mathbf{r}, t) &= \frac{\partial \mathbf{v}_0(\mathbf{r} - \mathbf{V}t, t)}{\partial t} + ((\mathbf{v}_0(\mathbf{r} - \mathbf{V}t, t) + \mathbf{V}).\nabla)(\mathbf{v}_0(\mathbf{r} - \mathbf{V}t, t) + \mathbf{V}), \\
&= \left. \frac{\partial \mathbf{v}_0(\mathbf{r} - \mathbf{V}t', t)}{\partial t'} \right|_{t' \rightarrow t} + \mathbf{g}_0(\mathbf{r} - \mathbf{V}t, t) + (\mathbf{V}.\nabla)\mathbf{v}_0(\mathbf{r} - \mathbf{V}t, t), \\
&= -(\mathbf{V}.\nabla)\mathbf{v}_0(\mathbf{r} - \mathbf{V}t, t) + \mathbf{g}_0(\mathbf{r} - \mathbf{V}t, t) + (\mathbf{V}.\nabla)\mathbf{v}_0(\mathbf{r} - \mathbf{V}t, t), \\
&= \mathbf{g}_0(\mathbf{r} - \mathbf{V}t, t), \tag{57}
\end{aligned}
$$

as there is a key cancellation of two terms in (57), and (ii) clearly $C(\mathbf{v}_0(\mathbf{r} - \mathbf{V}t, t) + \mathbf{V}) = C(\mathbf{v}_0(\mathbf{r} - \mathbf{V}t, t))$, and so this term is also simply translated. Hence apart from the translation effect the acceleration is the same. Hence the velocity vector addition rule in (56) is valid for generating the vector flow field for the translating matter distribution. This is why the large absolute motion velocities of some 400 km/s do not interfer with the usual computation and observation of gravitational forces.

For Earth based gravitational phenomena the motion of the Earth takes place within the velocity in-flow towards the Sun, and the velocity sum rule (56) is only approximately valid as now $\mathbf{V} \rightarrow \mathbf{V}(\mathbf{r}, t)$ and no longer corresponds to uniform translation, and manifests turbulence. To be a valid approximation the inhomogeneity of $\mathbf{V}(\mathbf{r}, t)$ must be much smaller than that of $\mathbf{v}_0(\mathbf{r} - \mathbf{V}t, t)$, which it is, as the Earth's centripetal acceleration about the Sun is approximately 1/1000 that of the Earth's gravitational acceleration at the surface of the Earth. Nevertheless turbulence associated with the $C(\mathbf{v})$ term is apparent in experimental data. The validity of this approximation demonstrates that the detection of a cosmic absolute motion and the in-flow theory of gravity are consistent with the older methods of computing gravitational forces. This is why both the presence of the $C(\mathbf{v})$ term, the in-flow and the absolute motion have gone almost unnoticed in Earth based gravitational experiments, except for various anomalies; see section 2.11.

2.10   Gravitational In-Flow and the GPS

We show here that the new in-flow theory of gravity together with the observed absolute velocity of motion of the solar system through space are together compatible with the operation of the Global Positioning System (GPS). This turns out to be an almost trivial exercise. As usual in this system the effects of the Sun and Moon are neglected. Various effects need to be included as the system relies upon extremely accurate atomic clocks in the satellites forming the GPS constellation. Within both the new theory and general relativity these clocks are effected by both their speed and the gravitational effects of

the Earth. As well the orbits of these satellites and the trajectories of radio signals from the satellites need to be computed. For the moment we assume spherical symmetry for the Earth. The effects of non-sphericity will be discussed below. In general relativity the orbits and signalling time delays are determined by the use of the geodesic equation (38) and the Schwarzschild metric (40). However these two equations are equivalent to the orbital equation (16) and the velocity field (56), with a velocity $\mathbf{V}$ of absolute motion, and with the in-flow given by (6), noting the result in section 2.9. For EM signalling the elapsed time in (9) requires careful treatment. Hence the two systems are completely mathematically equivalent: the computations within the new system may most easily be considered by relating them to the mathematically equivalent general relativity formalism. There are nevertheless two possible differences between the two theories. One is their different treatment of the non-sphericity of the Earth particularly via the $C(\mathbf{v})$ term, and (2) the effects of the in-flow turbulence. It is possible that these effects could lead to new experimental comparisons of the two theories, as well as perhaps to an improved accuracy within the system if these new effects are large enough.

2.11   Gravitational Anomalies

As noted in section 2.1 Newton's Inverse Square Law of Gravitation may only be strictly valid in cases of spherical symmetry. The theory that gravitational effects arise from inhomogeneities in the quantum foam flow implies that there is no 'universal law of gravitation' because the inhomogeneities are determined by non-linear 'fluid equations' and the solutions have no form which could be described by a 'universal law'. Fundamentally there is no generic fluid flow behaviour. The Inverse Square Law is then only an approximation, with large deviations expected in the case of spiral galaxies. Nevertheless Newton's gravitational constant G will have a definite value as it quantifies the effective rate at which matter dissipates the information content of space.

From these considerations it follows that the measurement of the value of G will be difficult as the measurement of the forces between two of more objects, which is the usual method of measuring G, will depend on the geometry of the spatial positioning of these objects in a way not previously accounted for because the Newtonian Inverse Square Law has always been assumed, or in some case a specified change in the form of the law has been used. But in all cases a 'law' has been assumed, and this may have been the flaw in the analysis of data from such experiments. This implies that the value of G from such experiments will show some variability as a systematic effect has been neglected in analysing the experimental data, for in none of these experiments is spherical symmetry present. So experimental measurements of G should show an unexpected contextuality. As well the influence of surrounding matter has also not been properly accounted for. Of course any effects of turbulence in the inhomogeneities of the flow has presumably also never even been contemplated.

The first measurement of G was in 1798 by Cavendish using a torsional balance. As the precision of experiments increased over the years and a variety of techniques used the disparity between the values of G has actually increased. In 1998 CODATA increased the uncertainty in G from 0.013% to 0.15%. One indication of the contextuality is that

measurements of G produce values that differ by nearly 40 times their individual error estimates [26]. It is predicted that these G anomalies will only be resolved when the new theory of gravity is used in analysing the data from these experiments, and that these precision G experiments provide another opportunity to check the new theory of gravity.

3   Observations of Absolute Motion and In-Flow

Absolute motion is motion relative to space itself. Absolute motion suggests that space has some structure, and indeed evidence of such structure has been repeatedly discovered over the last 115 years. It turns out that Michelson and Morley in their historic experiment of 1887 did detect absolute motion, but rejected their own findings because using Galilean relativity the determined speed of some 8 km/s was less than the 30 km/s orbital speed of the Earth. The data was clearly indicating that the theory for the operation of the Michelson interferometer was not adequate. Rather than reaching this conclusion Michelson and Morley came to the incorrect conclusion that their results amounted to the failure to detect absolute motion. This had an enormous impact on the development of physics, for as is well known Einstein accepted the erroneous evidence for the absence of absolute motion effects in his reinterpretion of the then extant Lorentzian interpretation. By the time Miller had finally figured out how to use and properly analyse data from his Michelson interferometer absolute motion had become a forbidden concept within physics, as it still is at present. The experimental observations by Miller and others of absolute motion has continued to be scorned and rejected by the physics community. Fortunately as well as revealing absolute motion the experimental data also reveals evidence in support of a new theory of gravity.

3.1   Theory of the Michelson Interferometer

We now show for the first time in over 100 years how three key effects together permit the Michelson interferometer [11] to reveal the phenomenon of absolute motion when operating in the presence of a gas, with the third effect only discovered in 2002 [5]. The main outcome is the expression for the time difference for light travelling via the orthogonal arms,

$$\Delta t = k^2 \frac{L|\mathbf{v}_P|^2}{c^3} \cos(2(\theta - \psi)) + O(|\mathbf{v}_P|^4). \tag{58}$$

Here $\mathbf{v}_P$ is the projection of the absolute velocity $\mathbf{v}$ of the interferometer through the quantum-foam onto the plane of the interferometer, where the projected velocity vector $\mathbf{v}_P$ has azimuth angle ψ relative to the local meridian, and θ is the angle of one arm from that meridian, i.e. the arm has angle $\theta - \psi$ to the projected direction of motion. The k^2 factor is $k^2 = (n^2 - 1)$ where n is the refractive index of the gas through which the light passes, and where we have assumed that $n \approx 1^+$, L is the rest-frame length of each arm and c is the speed of light relative to the quantum foam in the absence of a gas. This expression requires considerable care in its derivation, and here only a simplified analysis will be given for the case when the arms are either parallel or orthogonal to the direction
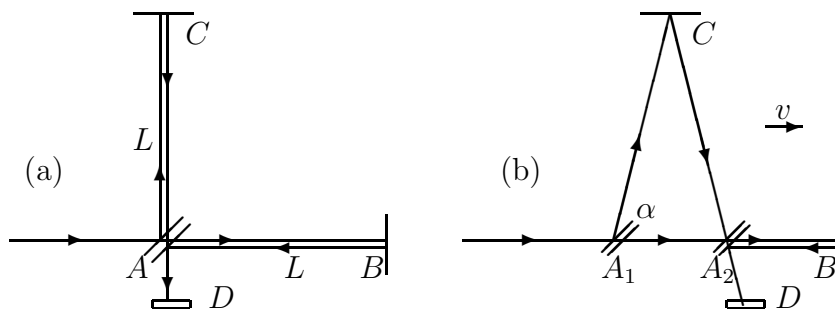
Figure 3: Schematic diagrams of the Michelson Interferometer, with beamsplitter/mirror at A and mirrors at B and C on arms from A, with the arms of equal length L when at rest. D is a quantum detector that causes localisation of the photon state by a collapse process. In (a) the interferometer is at rest in space. In (b) the interferometer is moving with speed v relative to space in the direction indicated. Interference fringes are observed at the quantum detector D. If the interferometer is rotated in the plane through 90°, the roles of arms AC and AB are interchanged, and during the rotation shifts of the fringes are seen in the case of absolute motion, but only if the apparatus operates in a gas. By counting fringe changes the speed v may be determined.

of motion and when the direction of motion is in the plane of the interferometer. The expression in (58) actually follows from three key effects: (i) the difference in geometrical length of the two paths when the interferometer is in absolute motion, as first realised by Michelson, (ii) the Fitzgerald-Lorentz contraction of the arms along the direction of motion, and (iii) that these two effects precisely cancel in vacuum, but leave a residual effect if operated in a gas, because the speed of light through the gas is reduced compared to vacuum. As well we shall take account of a fourth effect, namely the Fresnel drag in the gas caused by its absolute motion.

The time difference Δt is revealed by the fringe shifts on rotating the interferometer. However another effect needs to be considered. This time difference arises for light generated by atomic transitions in a light source that is travelling with the interferometer. And so there is a time dilation effect for this source. It turns out that fortunately because of the high speed and the direction of the observed absolute motion, compared to the orbital and in-flow velocities, that this effect is negligible as the change in the total v^2 over a year is sufficiently small. What is detected is the change in the projection of the total velocity onto the plane of the interferometer both during a day, and also seasonally due to the inclination of the plane of the ecliptic - the orbital plane, to the plane of motion of the interferometer due to the Earths daily rotation on its axis. However it should be noted that in the Kennedy-Thorndike [15] the effect of the absolute motion on the frequency of the light source was overlooked. This resulted in an erroneous analysis of data that was entirely instrumental noise.

In Newtonian physics, that is with no Fitzgerald-Lorentz contraction, $k^2 = n^3 \approx 1$ for gases, while in Einsteinian physics $k = 0$ reflecting the fundamental assumption that absolute motion is not measurable and indeed has no meaning. For air $n = 1.00029$,

and so $k = 0.0241$ and $k^2 = 0.00058$, which is close to the Einsteinian value of $k = 0$, particularly in comparison to the Newtonian value of $k = 1.0$. This small but non-zero k value explains why the Michelson interferometer experiments gave such small fringe shifts. Fortunately it is possible to check the n dependence of k as one experiment [9] was done in Helium gas, and this has an $n^2 - 1$ value significantly different from that of air.

As shown in figure 3 the beamsplitter/mirror when at A sends a photon $\psi(t)$ into a superposition $\psi(t) = \psi_1(t) + \psi_2(t)$, with each component travelling in different arms of the interferometer, until they are recombined in the quantum detector which results in a localisation process, and one spot in the detector is produced. Repeating with many photons reveals that the interference between ψ_1 and ψ_2 at the detector results in fringes. These fringes actually only appear if the mirrors are not quite orthogonal, otherwise the screen has a uniform intensity and this intensity changes as the interferometer is rotated, as shown in the analysis by Hicks [25]. To simplify the analysis here assume that the two arms are constructed to have the same lengths L when they are physically parallel to each other and perpendicular to v. Consider the Michelson interferometer operating in a gas which is moving with the interferometer at speed v. The motion of the gas relative to space results in a Fresnel drag effect. For simplicity consider only the cases when the arms are parallel/orthogonal to the direction of motion, as shown in figure 3. Let the arms have equal lengths L when at rest. The Fitzgerald-Lorentz relativistic effect is that the arm AB parallel to the direction of motion is shortened to

$$L_{\parallel} = L\sqrt{1 - \frac{v^2}{c^2}} \tag{59}$$

by absolute motion, while the length L of the transverse arm is unaffected. We work in the absolute rest frame. Consider the photon states in the AB arm. They travel at speed $V = c/n \pm bv$ relative to the quantum-foam which is space, where n is the refractive index of the gas and c is the speed of light in vacuum and relative to the space. Here $b = 1 - 1/n^2$ is the Fresnel drag coefficient which is well established experimentally. The motion of the gas through the quantum foam slightly 'drags' the light. The effect on the speed is $\pm bv$ depending on the direction of the light relative to the direction of absolute motion. Then the total travel time t_{ABA} is

$$t_{ABA} = t_{AB} + t_{BA} = \frac{L_{\parallel}}{\frac{c}{n} + bv - v} + \frac{L_{\parallel}}{\frac{c}{n} - bv + v} \tag{60}$$

$$= \frac{2Ln}{c}\sqrt{1 - \frac{v^2}{c^2}} \frac{1}{1 - \frac{v^2}{n^2c^2}}. \tag{61}$$

For the orthogonal arm we have by Pythagoras' theorem

$$(Vt_{AC})^2 = L^2 + (vt_{AC})^2. \tag{62}$$

The speed V of light travelling from A to C (and also from C to A) is

$$V = \frac{c}{n} + bv\cos(\alpha), \tag{63}$$

where α is the angle of the transverse light path to the direction of motion of the interferometer, as shown in figure 3, and is given by

$$\cos(\alpha) = \sqrt{1 - \frac{L^2}{(Vt)^2}}. \tag{64}$$

Solving (62), (63) and (64) for V we obtain

$$V = \frac{1}{2}\left(\frac{c^2}{n^2} + \sqrt{\frac{c^2}{n^2} + 4bv^2}\right). \tag{65}$$

Then (62) gives t_{AC}, and we obtain, with $t_{ACA} = t_{AC} + t_{CA} = 2t_{AC}$, and for $v \ll c$

$$\Delta t_{0^0 \to 90^0} = 2(t_{ABA} - t_{ACA}) = -2\frac{(n^2-1)(2-n^2)L}{nc}\frac{v^2}{c^2} + O(v^4), \tag{66}$$

for the change in relative travel times when the apparatus is rotated through 90^0. The factor of 2 arises because then the role of each arm is interchanged. For gases $n \approx 1^+$ and we obtain

$$\Delta t_{0^0 \to 90^0} \approx -2\frac{(n^2-1)L}{c}\frac{v^2}{c^2} + O(v^4). \tag{67}$$

A more general analysis shows that when the arm AB has angle $\theta - \psi$ relative to the projection of the velocity of absolute motion we obtain (58). Then on rotation through 90^0 the factor $\cos(2(\theta - \psi))$ changes by 2, so giving (58) the factor of 2 seen in (67). The major significance of this result is that this time difference is not zero when a gas is present in the interferometer, as confirmed by all gas-mode interferometer experiments. Of course this result also shows that vacuum-mode experiments, with $n = 1$, will give null results, as also confirmed by experiment [14, 15, 16, 17, 18]. So gas-mode Michelson interferometers are 'blind' to the effects of absolute motion, but they play a key role in confirming the Fitzgerald-Lorentz contraction effect, and by using vacuum they separate this effect from the refractive index effect.

It was Miller who first introduced the parameter k as he appreciated that the operation of the Michelson interferometer was not fully understood, although of course he never realised that k is related to the refractive index of the gas present in the interferometer. This is very fortunate since being a multiplicative parameter a re-scaling of old analyses is all that is required. Δt is non-zero when $n \neq 1$ because the refractive index effect results in incomplete cancellation between the geometrical effect and the Fitzgerald-Lorentz contraction effect. This incomplete cancellation arises whether we include the Fresnel drag effect or not, so its role in gas-mode Michelson interferometers is not critical. Leaving it out simply changes the overall sign in (58). Of course it was this cancellation effect that Fitzgerald and Lorentz actually used to arrive at the length contraction hypothesis, but they failed to take the next step and note that the cancellation would be incomplete in a gas operated Michelson interferometer. In a bizarre development modern Michelson interferometer experiments use resonant vacuum cavities rather than interference effects, but for which the analysis here is easily adapted, and

with the same consequences. That denies these experiments the opportunity to see absolute motion effects. Nevertheless the experimentalists continue to misinterpret their null results as evidence against absolute motion. Of course these experiments are therefore restricted to merely checking the Fitzgerald-Lorentz contraction effect, and this is itself of some interest.

All data from gas-mode interferometer experiments, except for that of Miller, has been incorrectly analysed using only the first effect as in Michelson's initial theoretical treatment, and so the consequences of the other two effects have been absent. Repeating the above analysis without these two effects we arrive at the Newtonian-physics time difference which, for $v << V$ and $n \approx 1^+$, is

$$\Delta t = L\frac{|\mathbf{v}_P|^2}{c^3}\cos(2(\theta - \psi)) + \mathrm{O}(|\mathbf{v}_P|^4), \tag{68}$$

that is $k = 1$. The value of Δt, which is typically of order $10^{-17} - 10^{-16}s$ in gas-mode interferometers corresponding to a fractional fringe shift, is deduced from analysing the fringe shifts, and then the speed v_M has been extracted using (68), instead of the correct form (67) (by the M subscript we indicate that the speed was obtained by using the incorrect Michelson theory (68)). However it is very easy to correct for this oversight. From (67) and (68) we obtain for the corrected absolute (projected) speed v_P through space, and for $n \approx 1^+$,

$$v_P = \frac{v_M}{\sqrt{n^2 - 1}}. \tag{69}$$

For air the correction factor in (69) is significant, and even more so for Helium.

3.2   The Michelson-Morley Experiment: 1887

Michelson and Morley reported that their interferometer experiment in 1887 gave a 'null-result' which since then, with rare exceptions, has been claimed to support the assumption that absolute motion has no meaning. However to the contrary the Michelson-Morley published data [7] shows non-null effects, but much smaller than they expected. They made observations of thirty-six 360^0 turns using an $L = 11$ meter length interferometer, achieved using multiple reflections, operating in air in Cleveland (Latitude 41^0 $30'$N) with six turns near $12:00$ hrs (7:00 hrs ST) on each day of July 8, 9 and 11, 1887 and similarly near $18:00$ hrs (13:00 hrs ST) on July 8, 9 and 12, 1887. Each turn took approximately 6 minutes as the interferometer slowly rotated floating on a tank of mercury. They published and analysed the average of each of the 6 data sets. The fringe shifts were extremely small but within their observational capabilities.

The orientation of the stone slab base is indicated by marks $16, 1, 2, ..$, as in figure 4; North is mark 16. The dominant effect was a uniform fringe drift caused by temporal temperature effects on the length of the arms, and imposed upon that are the fringe shifts corresponding to the effects of absolute motion, as shown in figure 4.

This temperature effect can be removed by subtracting from the data in each case a best fit to the data of $a + bk$, $\{k = 0, 1, 2, .., 8\}$ for the first 0^0 to 180^0 part of each rotation data set. Then multiplying by 0.02 for the micrometer thread calibration gives
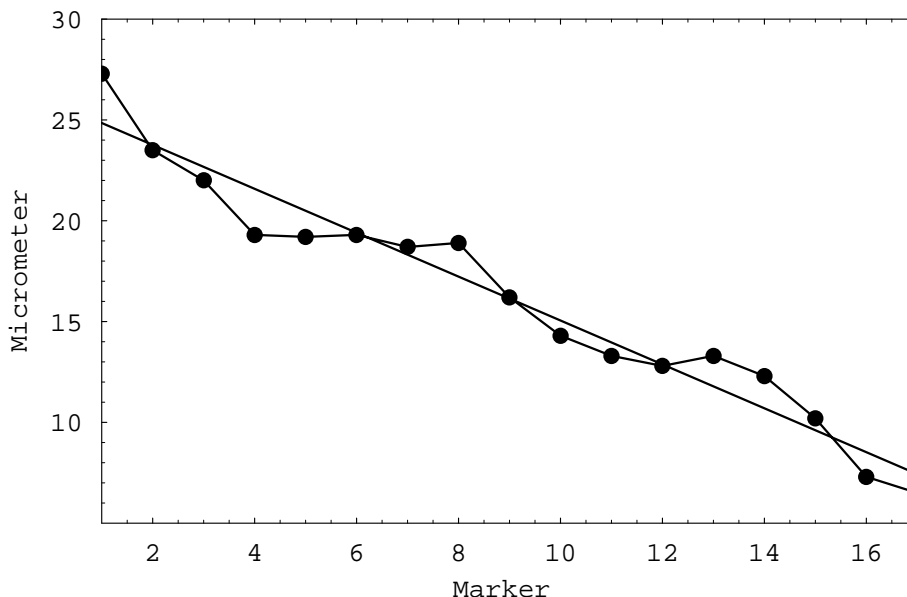
Figure 4: Plot of micrometer readings for July 11 12:00 hr (7:00 ST) showing the absolute motion induced fringe shifts superimposed on the uniform temperature induced fringe drift.

the fringe-shift data points in figure 6. This factor of 0.02 converts the micrometer readings to fringe shifts expressed as fractions of a wavelength. Similarly a linear fit has been made to the data from the 180^0 to 360^0 part of each rotation data set. Separating the full 360^0 rotation into two 180^0 parts reduces the effect of the temperature drift not being perfectly linear in time.

In the quantum-foam physics there are four main velocities that contribute to the total velocity:

$$\mathbf{v} = \mathbf{v}_{cosmic} + \mathbf{v}_{tangent} - \mathbf{v}_{in} - \mathbf{v}_E. \tag{70}$$

Here $\mathbf{v}_{cosmic}$ is the velocity of the Solar system through space, while the other three are local Solar system effects: (i) $\mathbf{v}_{tangent}$ is the tangential orbital velocity of the Earth about the Sun, (ii) $\mathbf{v}_{in}$ is a quantum-gravity radial in-flow of the quantum foam past the Earth towards the Sun, and (iii) the corresponding quantum-foam in-flow into the Earth is $\mathbf{v}_E$ and makes no contribution to a horizontally operated interferometer, assuming the velocity superposition approximation, and also that the turbulence associated with that flow is not significant. The minus signs in (70) arise because, for example, the in-flow towards the Sun requires the Earth to have an outward directed velocity against that in-flow in order to maintain a fixed distance from the Sun, as shown in figure 5. The superposition in (70) is justified by the analysis in section 2.9. For circular orbits $v_{tangent}$ and v_{in} are given by

$$v_{tangent} = \sqrt{\frac{GM}{R}}, \tag{71}$$

$$v_{in} = \sqrt{\frac{2GM}{R}}, \tag{72}$$

while the net speed v_N of the Earth from the vector sum $\mathbf{v}_N = \mathbf{v}_{tangent} - \mathbf{v}_{in}$ is

$$v_N = \sqrt{\frac{3GM}{R}}, \tag{73}$$

where M is the mass of the Sun, R is the distance of the Earth from the Sun, and G is Newton's gravitational constant. G is essentially a measure of the rate at which matter effectively 'dissipates' the quantum-foam. The gravitational acceleration arises from inhomogeneities in the flow. These expressions give $v_{tangent} = 30\text{km/s}$, $v_{in} = 42.4\text{km/s}$ and $v_N = 52\text{km/s}$.
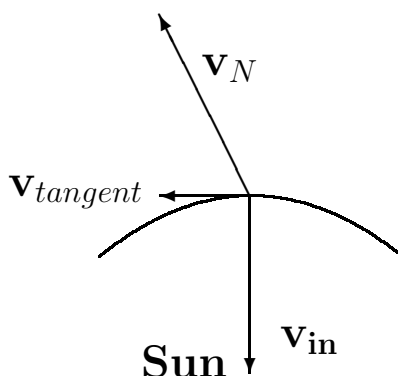

Figure 5: Orbit of Earth about the Sun defining the plane of the ecliptic with tangential orbital velocity $\mathbf{v}_{tangent}$ and quantum-foam in-flow velocity $\mathbf{v}_{in}$. Then $\mathbf{v}_N = \mathbf{v}_{tangent} - \mathbf{v}_{in}$ is the velocity of the Earth relative to the quantum foam, after subtracting $\mathbf{v}_{cosmic}$.

Figure 6 shows all the data for the 1887 Michelson-Morley experiment for the fringe shifts after removal of the temperature drift effect for each averaged 180 degree rotation. The dotted curves come from the best fit of $\frac{0.4}{30^2}k_{air}^2 v_P^2 \cos(2(\theta - \psi))$ to the data. The coefficient $0.4/30^2$ arises as the apparatus would give a 0.4 fringe shift, as a fraction of a wavelength, with $k = 1$ if $v_P = 30$ km/s [7]. Shown in each figure is the resulting value of v_P. In some cases the data does not have the expected $\cos(2(\theta - \psi))$ form, and so the corresponding values for v_P are not meaningful. The remaining fits give $v_P = 331 \pm 30$ km/s for the $7:00$ hr (ST) data, and $v_P = 328 \pm 50$ km/s for the $13:00$ hr (ST) data. For comparison the full curves show the predicted form for the Michelson-Morley data, computed for the latitude of Cleveland, using the Miller direction (see later) for $\mathbf{v}_{cosmic}$ of Right Ascension $\alpha = 4^{hr}\ 54'$ and Declination $\delta = -70^0\ 30'$ and incorporating the tangential and in-flow velocity effects for July. The magnitude of the theoretical curves are in general in good agreement with the magnitudes of the experimental data, excluding those cases where the data does not have the sinusoidal form. However there
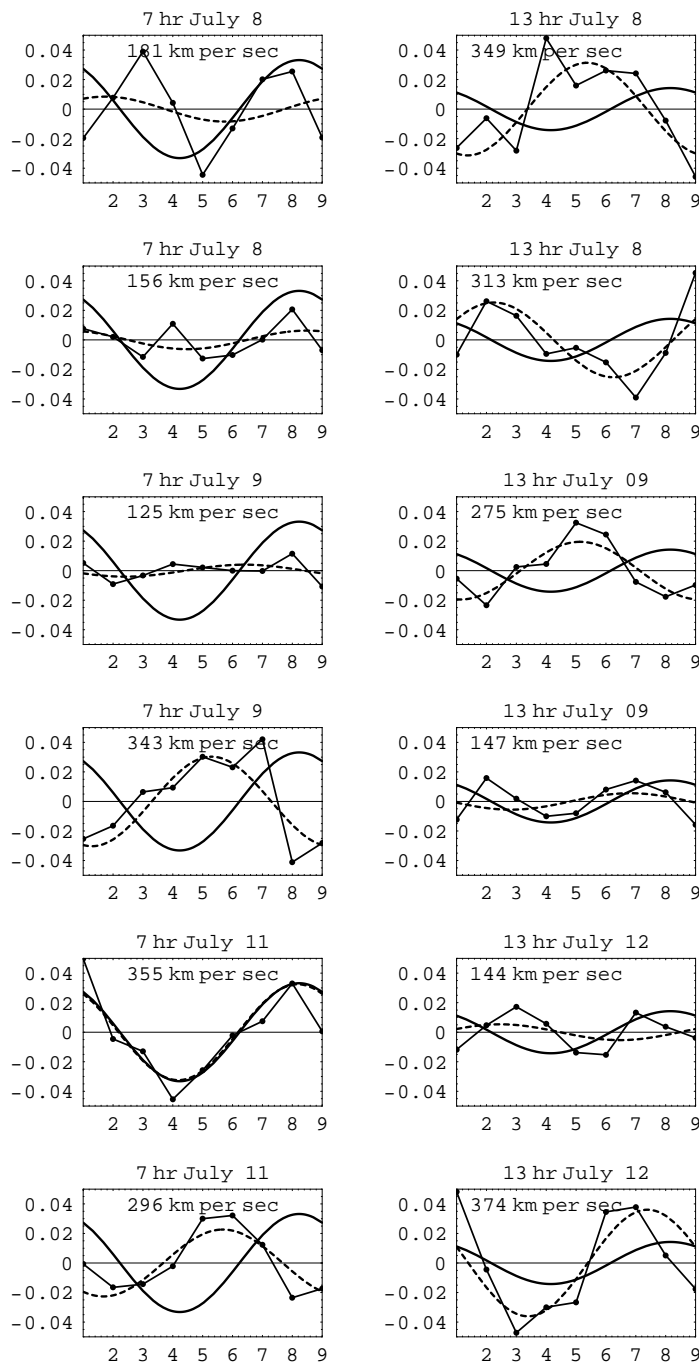
Figure 6: Shows all the Michelson-Morley 1887 data after removal of the temperature induced fringe drifts. The data for each 360^0 full turn (the average of 6 individual turns) is divided into the 1st and 2nd 180^0 parts and plotted one above the other. The dotted curve shows a best fit to the data, while the full curves show the expected forms using the Miller value for $\mathbf{v}_{cosmic}$, the tangential velocity and the in-flow velocity effect.

are significant fluctuations in the azimuth angle. These fluctuations are also present in the Miller data, and together suggest that this is a real physical phenomenon, and not solely due to difficulties with the operation of the interferometers.

The Michelson-Morley interferometer data clearly shows the characteristic sinusoidal form with period 180^0 together with a large speed. Ignoring the effect of the refractive index, namely using the Newtonian value of $k = 1$, gives speeds reduced by the factor k_{air}, namely $k_{air} v_P = 0.0241 \times 330 \text{km/s} = 7.9$ km/s. Michelson and Morley reported speeds in the range 5km/s - 7.5km/s. These slightly smaller speeds arise because they averaged all the 7:00 hr (ST) data, and separately all the 13:00 hr (ST) data, whereas here some of the lower quality data has not been used. Michelson was led to the false conclusion that because this speed of some 8 km/s was considerably less than the orbital speed of 30 km/s the interferometer must have failed to have detected absolute motion, and that the data was merely caused by experimental imperfections. This was the flawed analysis that led to the incorrect conclusion by Michelson and Morley that the experiment had failed to detect absolute motion. The consequences for physics were extremely damaging, and are only now being rectified after some 115 years.

3.3   The Miller Interferometer Experiment: 1925-1926

Dayton Miller developed and operated a Michelson interferometer for over twenty years with an effective arm length of $L = 32$m achieved by multiple reflections. The steel arms weighed 1200 kilograms and floated in a tank of 275 kilograms of Mercury. The main sequence of observations being on Mt.Wilson in the years 1925-1926, with the results reported in 1933 by Miller [8]. Miller developed his huge interferometer over the years, from 1902 to 1906 in collaboration with Morley, and later at Mt.Wilson where the most extensive interferometer observations were carried out. Miller was meticulous in perfecting the operation of the interferometer and performed many control experiments. The biggest problem to be controlled was the effect of temperature changes on the lengths of the arms. It was essential that the temperature effects were kept as small as possible but, so long as each turn was performed sufficiently quickly, any temperature effect could be assumed to have been linear with respect to the angle of rotation. Then a uniform background fringe drift could be removed, as in the Michelson-Morley data analysis (see figure 4).

In all some 200,000 readings were taken during some 12,000 turns of the interferometer. Analysis of the data involved the extraction of the speed v_M and the azimuth angle ψ by effectively fitting the observed time differences, obtained from the observed fringe shifts, using (68), i.e. with $k = 1$. Miller was of course unaware of the full theory of the interferometer and so he assumed the Newtonian theory, which neglected both the Fitzgerald-Lorentz contraction and the refractive index effects of the air effects.

Miller's results for April, August and September 1925 and February 1926 are shown in figure 7. Here the speeds shown are the proper speeds v_P after correcting for the refractive index effect, that is, by dividing Miller's v_M data values by $k_{air} = \sqrt{(n^2 - 1)} = 0.0241$, as in (69). Then for example a speed of $v_M = 10 km/s$ gives $v_P = v_M/k_{air} = 415$km/s. The Miller data was rediscovered in 2002 at Case Western Reserve University, and that data

has been used in preparing figure 7. However this refractive index correction procedure was not available to Miller. He understood that the theory of the Michelson interferometer was not complete, and so he introduced the phenomenological parameter k in (58). We shall denote his values by $\overline{k}$. Miller then proceeded on the assumption that $\mathbf{v}$ should have only two components: (i) a cosmic velocity of the Solar system through space, and (ii) the orbital velocity of the Earth about the Sun. Over a year this vector sum would result in a changing $\mathbf{v}$, as was in fact observed, see figure 7. Further, since the orbital speed was known, Miller was able to extract from the data the magnitude and direction of $\mathbf{v}$ as the orbital speed offered an absolute scale. For example the dip in the v_P plots for sidereal times $\tau \approx 16^{hr}$ is a clear indication of the direction of $\mathbf{v}$, as the dip arises at those sidereal times when the projection v_P of $\mathbf{v}$ onto the plane of the interferometer is at a minimum. During a 24hr period the value of v_P varies due to the Earth's rotation. As well the v_P plots vary throughout the year because the vectorial sum of the Earth's orbital velocity $\mathbf{v}_{tangent}$ and the cosmic velocity $\mathbf{v}_{cosmic}$ changes. There are two effects here as the direction of $\mathbf{v}_{tangent}$ is determined by both the yearly progression of the Earth in its orbit about the Sun, and also because the plane of the ecliptic is inclined at 23.5^0 to the celestial plane. Figure 8 show the expected theoretical variation of both v_P and the azimuth ψ during one sidereal day in the months of April, August, September and February. These plots show the clear signature of absolute motion effects as seen in the actual interferometer data of figure 7.

Note that the above corrected Miller projected absolute speed of approximately $v_P = 415$km/s is completely consistent with the corrected projected absolute speed of some 330km/s from the Michelson-Morley experiment, though neither Michelson nor Miller were able to apply this correction. The difference in magnitude is completely explained by Cleveland having a higher latitude than Mt.Wilson, and also by the only two sidereal times of the Michelson-Morley observations. So from his 1925-1926 observations Miller had completely confirmed the true validity of the Michelson-Morley observations and was able to conclude, contrary to their published conclusions, that the 1887 experiment had in fact detected absolute motion. But it was too late. By then the physicists had incorrectly come to believe that absolute motion was inconsistent with various 'relativistic effects' that had by then been observed. This was because the special relativity formalism had been 'derived' from the assumption that absolute motion was without meaning and so unobservable in principle. Of course the earlier interpretation of relativistic effects by Lorentz had by then lost out to this misunderstanding.

3.4 In-flow from the Miller Data

As already noted Miller was led to the conclusion that for reasons unknown the existing theory of the Michelson interferometer did not reveal true values of v_P, and for this reason he introduced the parameter k, with $\overline{k}$ indicating his numerical values. Miller had reasoned that he could determine both $\mathbf{v}_{cosmic}$ and $\overline{k}$ by observing the interferometer determined v_P and ψ over a year because the known orbital velocity of the Earth about the Sun would modulate both of these observables, and by a scaling argument he could determine the absolute velocity of the Solar system. In this manner he finally determined
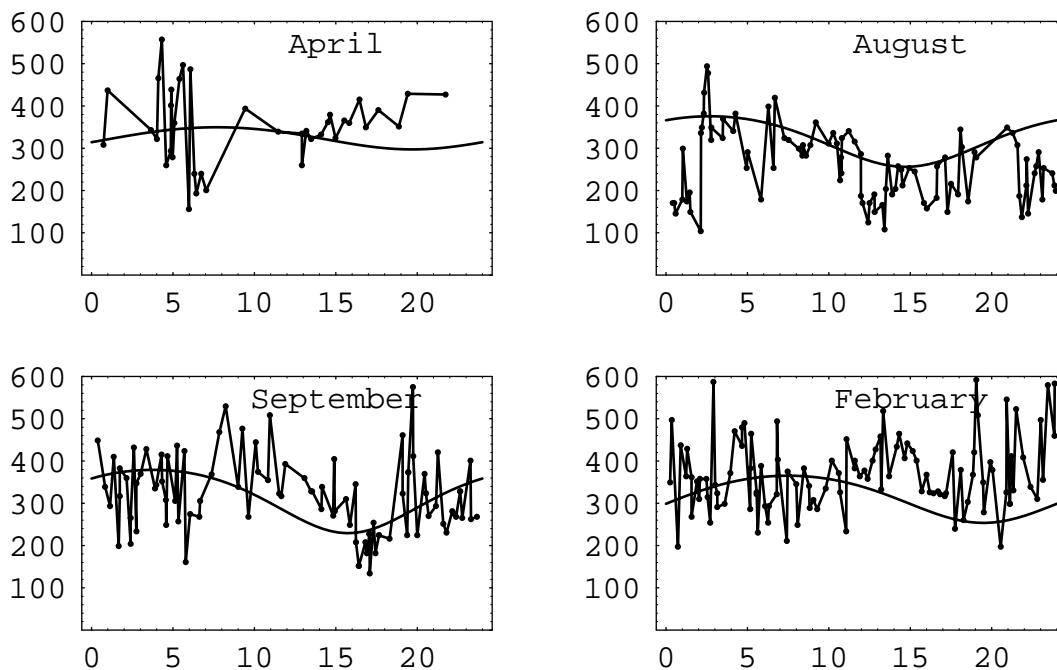
Figure 7: Miller's results from the 1925-1926 observations of absolute motion showing the projected speed v_P in km/s plotted against sidereal time in hours, after applying the refractive index correction (69). The results are for April, August and September 1925 and February 1926. In most cases the results arise from observations extending over much of each month, i.e not from a single day in each month. Therefore the data points are not strictly in chronological order. The lines joining the data points are merely to make the data points clearer. The fluctuations in both v_P, and in ψ (not shown) appear to be a combination of apparatus effects and genuine physical phenomena caused by turbulence in the gravitational in-flow of space towards the Sun. Each data point arises from analysis of the average of twenty full rotations of the interferometer. The theoretical curves, which include the cosmic velocity, the tangential orbital velocity and the in-flow effect, are shown for $v_c = 420$km/s and ($\alpha = 4^{hr}, \delta = -80^0$), and are assembled in one plot in figure 8 to display more clearly the diurnal and seasonal variations.

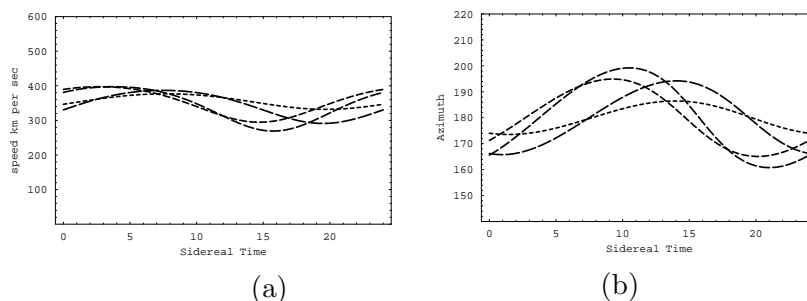Figure 8: Expected theoretical variation of (a) the projected velocity v_P, and (b) the azimuth ψ during one sidereal day in the months of April, August, September and February, labelled by increasing dash length. These forms arise from a best fit to the data in figure 7. The cosmic speed is 420km/s in the direction $(\alpha = 5^{hr}, \delta = -80^0)$, and the tangential and in-flows velocities are as in (70). These plots show the characteristics of the signature expected in observations of absolute motion.

that $|\mathbf{v}_{cosmic}| = 208$ km/s in the direction $(\alpha = 4^{hr}\ 54^m, \delta = -70^0\ 33')$. However now that the theory of the Michelson interferometer has been revealed an anomaly becomes apparent. Table 3 shows $v = v_M/k_{air}$ for each of the four epochs, giving speeds consistent with the revised Michelson-Morley data. However table 3 also shows that $\overline{k}$ and the speeds $\overline{v} = v_M/\overline{k}$ determined by the scaling argument are considerably different. Here the v_M values arise after taking account of the projection effect. That $\overline{k}$ is considerably larger than the value of k_{air} indicates that another velocity component has been overlooked. Miller of course only knew of the tangential orbital speed of the Earth, whereas the new quantum foam physics predicts that as-well there is a quantum-gravity radial in-flow $\mathbf{v}_{in}$ of the quantum foam. We can re-analyse Miller's data to extract a first approximation to the speed of this in-flow component. Clearly it is $v_N = \sqrt{v_{in}^2 + v_{tangent}^2}$ that sets the scale and not $v_{tangent}$, and because $\overline{k} = v_M/v_{tangent}$ and $k_{air} = v_M/v_N$ are the scaling relations, then

$$
\begin{aligned}
v_{in} &= v_{tangent}\sqrt{\frac{v_N^2}{v_{tangent}^2} - 1}, \\
&= v_{tangent}\sqrt{\frac{\overline{k}^2}{k_{air}^2} - 1}.
\end{aligned}
\tag{74}
$$

Using the $\overline{k}$ values in table 3 and the value of k_{air} we obtain the v_{in} speeds shown in table 3, which give an average speed of 54 km/s, compared to the 'Newtonian' in-flow speed of 42 km/s. Note that the in-flow interpretation of the anomaly predicts that $\overline{k} = (v_N/v_{tangent})\,k_{air} = \sqrt{3}\,k_{air} = 0.042$. Of course this simple re-scaling of the Miller results is not completely valid because (i) the direction of $\mathbf{v}_N$ is of course different to that of $\mathbf{v}_{tangent}$, and also not necessarily orthogonal to $\mathbf{v}_{tangent}$ because of turbulence, and (ii) also because of turbulence we would expect some contribution from the in-flow

Epoch	v_M	$\overline{k}$	$v = v_M/k_{air}$	$\overline{v} = v_M/\overline{k}$	$v = \sqrt{3}\overline{v}$	v_{in}
February 8	9.3 km/s	0.048	385.9 km/s	193.8 km/s	335.7 km/s	51.7 km/s
April 1	10.1	0.051	419.1	198.0	342.9	56.0
August 1	11.2	0.053	464.7	211.3	366.0	58.8
September 15	9.6	0.046	398.3	208.7	361.5	48.8

Table 3. The $\overline{k}$ anomaly: $\overline{k} \gg k_{air} = 0.0241$, as the gravitational in-flow effect. Here v_M and $\overline{k}$ come from fitting the interferometer data, while v and $\overline{v}$ are computed speeds using the indicated scaling. The average of the in-flow speeds is $v_{in} = 54 \pm 5$ km/s, compared to the 'Newtonian' in-flow speed of 42 km/s. From column 4 we obtain the average $v = 417 \pm 40$km/s. A fit to the Miller speed data gives the curves in figures 7 and 8.

effect of the Earth itself, which has a speed of 11 km/s, namely that it is not always perpendicular to the Earth's surface, and so would give a contribution to a horizontally operated interferometer.

An analysis that properly searches for the in-flow velocity effect clearly requires a complete re-analysis of the Miller data, and this is now possible as the original data sheets have been found. In figures 7 and 8 the results of a preliminary re-fit are shown, but a more extensive one is in progress. It should be noted that the direction diametrically opposite ($\alpha = 4^{hr}\ 54^m, \delta = -70^0\ 33'$), namely ($\alpha = 17^{hr}, \delta = +68'$) was at one stage considered by Miller as being possible. This is because the Michelson interferometer, being a 2nd-order device, has a directional ambiguity which can only be resolved by using the seasonal motion of the Earth. However as Miller did not include the in-flow velocity effect in his analysis it is possible that a re-analysis might give this northerly direction as the direction of absolute motion of the Solar system.

Hence not only did Miller observe absolute motion, as he claimed, but the quality and quantity of his data has also enabled the confirmation of the existence of the gravitational in-flow effect. This is a manifestation of the new theory of gravity and one which relates to quantum gravitational effects via the unification of matter and space developed in [1]. As well the persistent evidence that this in-flow is turbulent indicates that this theory of gravity involves self-interaction of space itself.

3.5   The Illingworth Experiment: 1927

In 1927 Illingworth [9] performed a Michelson interferometer experiment in which the light beams passed through the gas Helium. Helium was used in the interferometer to in fact reduce the temperature effects via any refractive index effects, as a good vacuum was difficult to achieve. For Helium at STP $n = 1.000036$ and so $k_{He}^2 = 0.00007$, which results in an enormous reduction in sensitivity of the interferometer. Nevertheless this experiment gives an excellent opportunity to check the n dependence in (69). Illingworth, not surprisingly, reported no "ether drift to an accuracy of about one kilometer per second". Múnera [27] re-analysed the Illingworth data to obtain a speed $v_M = 3.13 \pm 1.04$km/s. The correction factor in (69), $1/\sqrt{n_{He}^2 - 1} = 118$, is large for Helium and gives $v = 368 \pm 123$km/s. As shown in figure 9 the Illingworth observations now agree
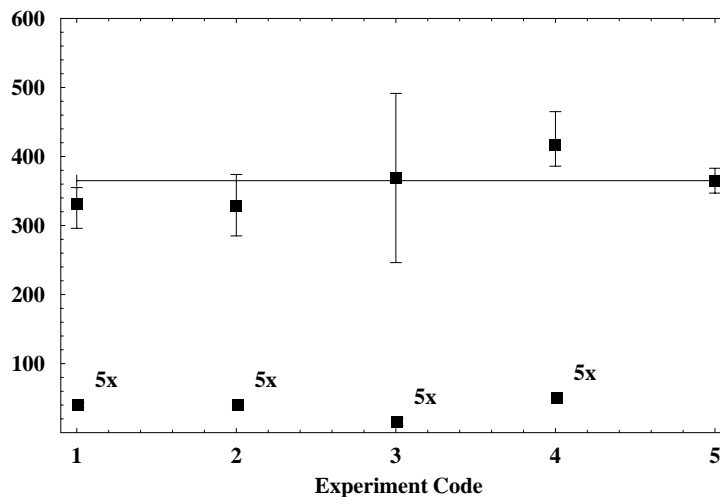
Figure 9: Speeds v in km/s determined from various Michelson interferometer experiments (**1**)-(**4**) and CMB (**5**): (**1**) Michelson-Morley (noon observations) and (**2**) (18^h observations) see section 3.2, (**3**) Illingworth [9], (**4**) Miller, Mt.Wilson [8], and finally in (**5**) the speed from observations of the CMB spectrum dipole term [19]. The results (**1**)-(**3**) are not corrected for the ± 30km/s of the orbital motion of the Earth about the Sun or for the gravitational in-flow speed, though these correction were made for (**4**) with the speeds from table 3. The horizontal line at $v = 369$km/s is to aid comparisons with the CMB frame speed data. The Miller direction is different to the CMB direction. Due to the angle between the velocity vector and the plane of interferometer the results (**1**)-(**3**) are less than or equal to the true speed, while the result for (**4**) is the true speed as this projection effect was included in the analysis. These results demonstrate the remarkable consistency between the three interferometer experiments. The Miller speed agrees with the speed from the DeWitte non-interferometer experiment, in section 3.7. The lower data, magnified by a factor of 5, are the original speeds v_M determined from fringe shifts using (58) with $k = 1$. This figure updates the corresponding figure in reference [5].

with those of Michelson-Morley and Miller, though they would certainly be inconsistent without the $n-$dependent correction, as shown in the lower data points (shown at $5\times$ scale).

So the use by Illingworth of Helium gas has turned out have offered a fortuitous opportunity to confirm the validity of the refractive index effect, though because of the insensitivity of this experiment the resulting error range is significantly larger than those of the other interferometer observations. So finally it is seen that the Illingworth experiment also detected absolute motion with a speed consistent with all other observations.

3.6 The New Bedford Experiment: 1963

In 1964 from an absolute motion detector experiment at New Bedford, latitude 42^0N, Jaseja *et al* [10] reported yet another 'null result'. In this experiment two He-Ne masers were mounted with axes perpendicular on a rotating table, see figure 10. Rotation of the table through 90^0 produced repeatable variations in the frequency difference of about 275kHz, an effect attributed to magnetorestriction in the Invar spacers due to the Earth's magnetic field. Observations over some six consecutive hours on January 20, 1963 from $6\!:\!00$ am to $12\!:\!00$ noon local time did produce a 'dip' in the frequency difference of some 3kHz superimposed on the 275kHz effect, as shown in figure 11 in which the local times have been converted to sidereal times. The most noticeable feature is that the dip occurs at approximately $17 - 18\!:\!00^{hr}$ sidereal time (or $9 - 10\!:\!00$ hrs local time), which agrees with the direction of absolute motion observed by Miller and also by DeWitte (see section 3.7). It was most fortunate that this particular time period was chosen as at other times the effect is much smaller, as shown for example for the February data in figure 7. The local times were chosen by Jaseja *et al* such that if the only motion was due to the Earth's orbital speed the maximum frequency difference, on rotation, should have occurred at 12:00hr local time, and the minimum frequency difference at 6:00 hr local time, whereas in fact the minimum frequency difference occurred at 9:00 hr local time.

As for the Michelson-Morley experiment the analysis of the New Bedford experiment was also bungled. Again this apparatus can only detect the effects of absolute motion if the cancellation between the geometrical effects and Fitzgerald-Lorentz length contraction effects is incomplete as occurs only when the radiation travels in a gas, here the He-Ne gas present in the maser.

This double maser apparatus is essentially equivalent to a Michelson interferometer. Then the resonant frequency ν of each maser is proportional to the reciprocal of the out-and-back travel time. For maser 1

$$\nu_1 = m\frac{V^2 - v^2}{2LV\sqrt{1 - \dfrac{v^2}{c^2}}}, \tag{75}$$

for which a Fitzgerald-Lorentz contraction occurs, while for maser 2

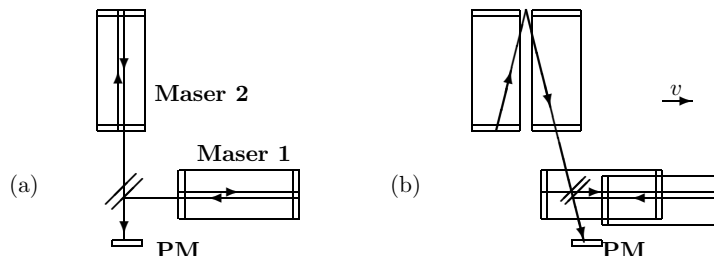$$\nu_2 = m\frac{\sqrt{V^2 - v^2}}{2L}. \tag{76}$$

Figure 10: Schematic diagram for recording the variations in beat frequency between two optical masers: (a) when at absolute rest, (b) when in absolute motion at velocity **v**. PM is the photomultiplier detector. The apparatus was rotated back and forth through 90^0.

Here m refers to the mode number of the masers. When the apparatus is rotated the net observed frequency difference is $\delta\nu = 2(\nu_2 - \nu_1)$, where the factor of '2' arises as the roles of the two masers are reversed after a 90^0 rotation. Putting $V = c/n$ we find for $v << V$ and with ν_0 the at-rest resonant frequency, that

$$\delta\nu = (n^2 - 1)\nu_0 \frac{v^2}{c^2} + O(\frac{v^4}{c^4}). \tag{77}$$

Including Fresenl drag in the masers changes the sign in (77), and so has no effect on the analysis here. If we use the Newtonian physics analysis, as in Jaseja *et al* [10], which neglects both the Fitzgerald-Lorentz contraction and the refractive index effect, then we obtain $\delta\nu = \nu_0 v^2/c^2$, that is without the $n^2 - 1$ term, just as for the Newtonian analysis of the Michelson interferometer itself. Of course the very small magnitude of the absolute motion effect, which was approximately 1/1000 that expected assuming only an orbital speed of $v = 30$ km/s in the Newtonian analysis, occurs simply because the refractive index of the He-Ne gas is very close to one. It is possible to compare the refractive index of the He-Ne gas mixture in the maser with the value extractable from this data: $n^2 = 1 + 30^2/(1000 \times 400^2)$, or $n = 1.0000028$. Nevertheless given that it is small the sidereal time of the obvious 'dip' coincides almost exactly with that of the other observations of absolute motion.

The New Bedford experiment was yet another missed opportunity to have revealed the existence of absolute motion. Again the spurious argument was that because the Newtonian physics analysis gave the wrong prediction then the vacuum special relativity must be correct. But the analysis simply failed to take account of the Fitzgerald-Lorentz contraction, which had been known since the end of the 19th century. As well the authors failed to convert their local times to sidereal times and compare the time for the 'dip' with Miller's time.
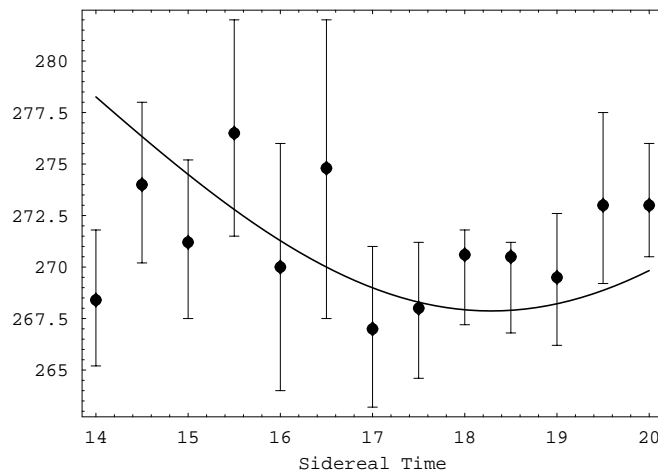
Figure 11: Frequency difference in kHz between the two masers in the 1963 New Bedford experiment after a 90^0 rotation. The 275kHz difference is a systematic repeatable apparatus effect, whereas the superimposed 'dip' at $17 - 18{:}00^{hr}$ sidereal time of approximately 3kHz is a real time dependent frequency difference. The full curve shows the theoretical prediction for the time of the 'dip' for this experiment using the Miller direction for $\hat{\mathbf{v}}$ ($\alpha = 4^{hr}54^m, \delta = -70^0 33'$) with $|\mathbf{v}| = 417$km/s and including the Earth's orbital velocity and Sun gravitational in-flow velocity effects for January 20, 1963. The absolute scale of this theoretical prediction was not possible to compute as the refractive index of the He-Ne gas mixture was unknown.

3.7   The DeWitte Experiment: 1991

The Michelson-Morley, Illingworth, Miller and New Bedford experiments all used Michelson interferometers or its equivalent in gas mode, and all revealed absolute motion. The Michelson interferometer is a 2nd-order device meaning that the time difference between the 'arms' is proportional to $(v/c)^2$. There is also a factor of $n^2 - 1$ and for gases like air and particularly Helium or Helium-Neon mixes this results in very small time differences and so these experiments were always very difficult. Of course without the gas the Michelson interferometer is incapable of detecting absolute motion, and so there are fundamental limitations to the use of this interferometer in the study of absolute motion and related effects.

In a remarkable development in 1991 a research project within Belgacom, the Belgium telecommunications company, stumbled across yet another detection of absolute motion, and one which turned out to be 1st-order in v/c. The study was undertaken by Roland DeWitte [13]. This organisation had two sets of atomic clocks in two buildings in Brussels separated by 1.5 km and the research project was an investigation of the task of synchronising these two clusters of atomic clocks. To that end 5MHz radiofrequency signals were sent in both directions through two buried coaxial cables linking the two clusters. The atomic clocks were caesium beam atomic clocks, and there were three in each cluster. In that way the stability of the clocks could be monitored. One cluster was
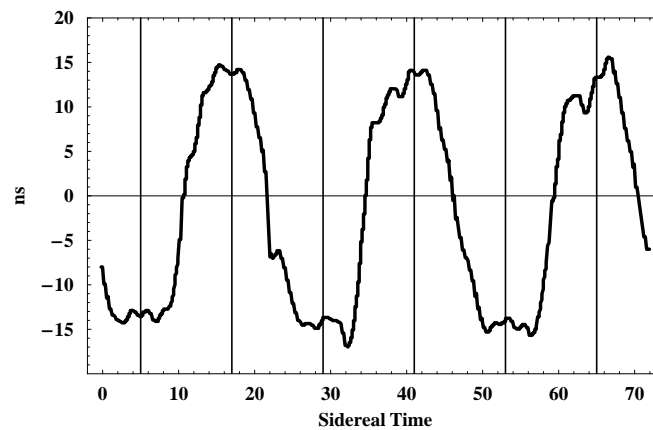
Figure 12: Variations in twice the one-way travel time, in ns, for an RF signal to travel 1.5 km through a coaxial cable between Rue du Marais and Rue de la Paille, Brussels. An offset has been used such that the average is zero. The definition of the sign convention for Δt used by DeWitte is unclear. The cable has a North-South orientation, and the data is $\pm$ difference of the travel times for NS and SN propagation. The sidereal time for maximum effect of $\sim$17hr (or $\sim$5hr) (indicated by vertical lines) agrees with the direction found by Miller and also by Jaseja et al, but because of the ambiguity in the definition of Δt the opposite direction would also be consistent with this data. Plot shows data over 3 sidereal days and is plotted against sidereal time. See figure 13b for theoretical predictions for one sidereal day. The time of the year of the data is not identified. The fluctuations are evidence of turbulence associated with the gravitational in-flow towards the Sun. Adapted from DeWitte [13].
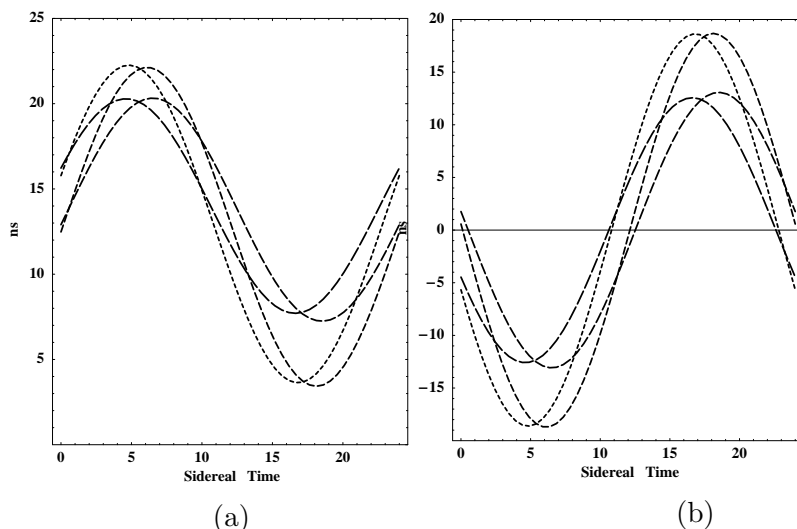
Figure 13: Theoretical predictions for the variations in travel time, in ns, for one sidereal day, in the DeWitte Brussels coaxial cable experiment for $\mathbf{v}_{cosmic}$ in the direction $(\alpha, \delta) = (17.5^h, 65^0)$ and with the Miller magnitude of 417 km/s, and including orbital and in-flow effects (but without turbulence). Shown are the results for four days: for the Vernal Equinox, March 21 (shortest dashes), and for 90, 180 and 270 days later (shown with increasing dash length). Figure (a) Shows change in one-way travel time $t_0 n v_P / c$ for signal travelling from N to S. Figure (b) shows Δt, as defined in (78), with an offset such that the average is zero so as to enable comparison with the data in figure 12. Δt is twice the one-way travel time. For the direction opposite to $(\alpha, \delta) = (17.5^h, 65^0)$ the same curves arise except that the identification of the months is different and the sign of Δt also changes. The sign of Δt determines which of the two directions is the actual direction of absolute motion. However the definition of the sign convention for Δt used by DeWitte is unclear.

in a building on Rue du Marais and the second cluster was due south in a building on Rue de la Paille. Digital phase comparators were used to measure changes in times between clocks within the same cluster and also in the propagation times of the RF signals. Time differences between clocks within the same cluster showed a linear phase drift caused by the clocks not having exactly the same frequency together with short term and long term noise. However the long term drift was very linear and reproducible, and that drift could be allowed for in analysing time differences in the propagation times between the clusters.

Changes in propagation times were observed and eventually observations over 178 days were recorded. A sample of the data, plotted against sidereal time for just three days, is shown in figure 12. DeWitte recognised that the data was evidence of absolute motion but he was unaware of the Miller experiment and did not realise that the Right Ascension for maximum/minimum propagation time agreed almost exactly with Miller's direction $(\alpha, \delta) = (17.5^h, 65^0)$. In fact DeWitte expected that the direction of absolute

motion should have been in the CMB direction, but that would have given the data a totally different sidereal time signature, namely the times for maximum/minimum would have been shifted by 6 hrs. The declination of the velocity observed in this DeWitte experiment cannot be determined from the data as only three days of data are available. However assuming exactly the same declination as Miller the speed observed by DeWitte appears to be also in excellent agreement with the Miller speed, which in turn is in agreement with that from the Michelson-Morley and Illingworth experiments, as shown in figure 9.

Being 1st-order in v/c the Belgacom experiment is easily analysed to sufficient accuracy by ignoring relativistic effects, which are 2nd-order in v/c. Let the projection of the absolute velocity vector $\mathbf{v}$ onto the direction of the coaxial cable be v_P as before. Then the phase comparators reveal the difference between the propagation times in NS and SN directions. First consider the analysis with no Fresnel drag effect,

$$
\begin{aligned}
\Delta t &= \frac{L}{\dfrac{c}{n} - v_P} - \frac{L}{\dfrac{c}{n} + v_P}, \\
&= 2\frac{L}{c/n}n\frac{v_P}{c} + O(\frac{v_P^2}{c^2}) \approx 2t_0 n\frac{v_P}{c}.
\end{aligned} \tag{78}
$$

Here $L = 1.5$ km is the length of the coaxial cable, $n = 1.5$ is the refractive index of the insulator within the coaxial cable, so that the speed of the RF signals is approximately $c/n = 200,000$km/s, and so $t_0 = nL/c = 7.5 \times 10^{-6}$ sec is the one-way RF travel time when $v_P = 0$. Then, for example, a value of $v_P = 400$km/s would give $\Delta t = 30$ns. Because Brussels has a latitude of 51^0 N then for the Miller direction the projection effect is such that v_P almost varies from zero to a maximum value of $|\mathbf{v}|$. The DeWitte data in figure 12 shows Δt plotted with a false zero, but shows a variation of some 28 ns. So the DeWitte data is in excellent agreement with the Miller's data. There is ambiguity in reference [13] as to whether the time variations in figure 12 include the factor of 2 or not, as defined in (78). It is assumed here that a factor of 2 is included. The Miller experiment has thus been confirmed by a non-interferometer experiment if we ignore a Fresnel drag.

But if we include a Fresnel drag effect then the change in travel time Δt_F becomes

$$
\begin{aligned}
\Delta t_F &= \frac{L}{\dfrac{c}{n} + bv_P - v_P} - \frac{L}{\dfrac{c}{n} - bv_P + v_P}, \\
&= 2\frac{L}{c}\frac{v_P}{c} + O(\frac{v_P^2}{c^2}), \\
&= \frac{1}{n^2}\Delta t,
\end{aligned} \tag{79}
$$

where $b = 1 - 1/n^2$ is the Fresnel drag coefficient. Then Δt_F is smaller than Δt by a factor of $n^2 = 1.5^2 = 2.25$, and so a speed of $v_P = 2.25 \times 400 = 900$ km/s would be required to produce a $\Delta t_F = 30$ ns. This speed is inconsistent with the results from gas-mode interferometer experiments. This raises the question as to whether the Fresnel

effect is present in transparent solids, and indeed whether it has ever been studied? As well we are assuming the conventional eletromagnetic theory for the RF fields in the coaxial cable. An experiment to investigate this is underway at Flinders university.

The actual days of the data in figure 12 are not revealed in reference [13] so a detailed analysis of the DeWitte data is not possible. Nevertheless theoretical predictions for various days in a year are shown in figure 13 using the Miller speed of $v_{cosmic} = 417$ km/s (from table 3) and where the diurnal effects of the Earth's orbital velocity and the gravitational in-flow cause the range of variation of Δt and sidereal time of maximum effect to vary throughout the year. The predictions give $\Delta t = 30 \pm 4$ ns over a year compared to the DeWitte value of 28 ns in figure 12. If all of DeWitte's 178 days of data were available then a detailed analysis would be possible.

Reference [13] does however reveal the sidereal time of the cross-over time, that is a 'zero' time in figure 12, for all 178 days of data. This is plotted in figure 14 and demonstrates that the time variations are correlated with sidereal time and not local solar time. A least squares best fit of a linear relation to that data gives that the cross-over time is retarded, on average, by 3.92 minutes per solar day. This is to be compared with the fact that a sidereal day is 3.93 minutes shorter than a solar day. So the effect is certainly cosmological and not associated with any daily thermal effects, which in any case would be very small as the cable is buried. Miller had also compared his data against sidereal time and established the same property namely that, up to small seasonal effects caused by the Earth's orbital plane being inclined to the equatorial plane, features in the data tracked sidereal time and not solar time; see reference [8] for a detailed analysis.

The DeWitte data is also capable of resolving the question of the absolute direction of motion found by Miller. Is the direction $(\alpha, \delta) = (17.5^h, 65^0)$ or the opposite direction? Being a 2nd-order Michelson interferometer experiment Miller had to rely on the Earth's seasonal effects in order to resolve this ambiguity, but his analysis of course did not take account of the gravitational in-flow effect, and so until a re-analysis of his data his preferred choice of direction must remain to be confirmed. The DeWitte experiment could easily resolve this ambiguity by simply noting the sign of Δt. Unfortunately it is unclear in reference [13] as to how the sign in figure 12 is actually defined, and DeWitte does not report a direction expecting, as he did, that the direction should have been the same as the CMB direction $(\alpha = 11.20^h, \delta = -7.22^0)$.

3.8 The Torr-Kolen Experiment: 1981

A coaxial cable experiment similar to but before the DeWitte experiment was performed at the Utah University in 1981 by Torr and Kolen [12]. This involved two rubidium vapor clocks placed approximately 500m apart with a 5 MHz sinewave RF signal propagating between the clocks via a nitrogen filled coaxial cable maintained at a constant pressure of ~2 psi. This means that the Fresnel drag effect is not important in this experiment. Unfortunately the cable was orientated in an East-West direction which is not a favourable orientation for observing absolute motion in the Miller direction, unlike the Brussels North-South cable orientation. There is no reference to Miller's result in the Torr and Kolen paper, otherwise they would presumably not have used this orientation. Never-
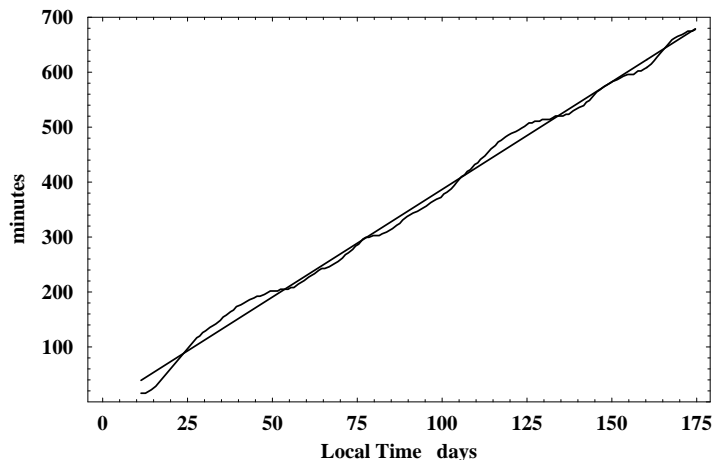
Figure 14: Plot of the negative of the drift of the cross-over time between minimum and maximum travel-time variation each day (at $\sim 10^h \pm 1^h$ ST) versus local solar time for some 180 days. The straight line plot is the least squares fit to the experimental data, giving an average slope of 3.92 minutes/day. The time difference between a sidereal day and a solar day is 3.93 minutes/day. This demonstrates that the effect is related to sidereal time and not local solar time. The actual days of the year are not identified in reference [13]. Adapted from DeWitte [13].

theless there is a projection of the absolute motion velocity onto the East-West cable and Torr and Kolen did observe an effect in that, while the round speed time remained constant within 0.0001%c, typical variations in the one-way travel time were observed, as shown in figure 15 by the data points. The theoretical predictions for the Torr-Kolen experiment for a cosmic speed of 417 km/s in the direction $(\alpha, \delta) = (17.5^h, 65^0)$, and including orbital and in-flow velocities, are shown in figure 15. As well the maximum effect occurred, typically, at the predicted times. So the results of this experiment are also in agreement with the Miller direction, and the speed of 417 km/s which of course only arises after re-scaling the Miller speeds for the effects of the gravitational in-flow. As well Torr and Kolen reported fluctuations in both the magnitude and time of the maximum variations in travel time just as DeWitte observed some 10 years later. Again we argue that these fluctuations are evidence of genuine turbulence in the in-flow as discussed in section 3.10. So the Torr-Kolen experiment again shows strong evidence for the new theory of gravity, and which is over and above its confirmation of the various observations of absolute motion.

3.9 Galactic In-flow and the CMB Frame

Absolute motion (AM) of the Solar system has been observed in the direction $(\alpha = 17.5^h, \delta = 65^0)$, up to an overall sign to be sorted out, with a speed of 417 ± 40 km/s. This is the velocity after removing the contribution of the Earth's orbital speed and the Sun in-flow effect. It is significant that this velocity is different to that associated with the
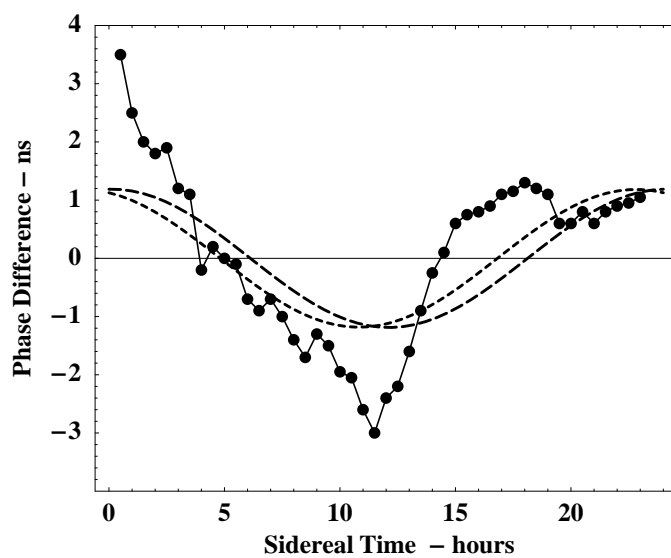
Figure 15: Data from the 1981 Torr-Kolen experiment at Logan, Utah [12]. The data shows variations in travel times (ns), for local times, of an RF signal travelling through 500m of coaxial cable orientated in an E-W direction. Actual days are not indicated but the experiment was done during February-June 1981. Results are for a typical day. For the 1st of February the local time of 12:00 corresponds to 13:00 sidereal time. The predictions are for March (shortest dashes) and June, for a cosmic speed of 417 km/s in the direction $(\alpha, \delta) = (17.5^h, 65^0)$, and including orbital and in-flow velocities but without theoretical turbulence.

Cosmic Microwave Background (CMB) relative to which the Solar system has a speed of 369 km/s in the direction ($\alpha = 11.20^h, \delta = -7.22^0$), see [19]. This CMB velocity is obtained by finding the preferred frame in which this thermalised 3^0K radiation is isotropic, that is by removing the dipole component. The CMB velocity is a measure of the motion of the Solar system relative to the universe as a whole, or atleast a shell of the universe some 14Gyrs away, and indeed the near uniformity of that radiation in all directions demonstrates that we may meaningfully refer to the spatial structure of the universe. The concept here is that at the time of decoupling of this radiation from matter that matter was on the whole, apart from small observable fluctuations, at rest with respect to the quantum-foam system that is space. So the CMB velocity is the motion of the Solar system with respect to space *universally*, but not necessarily with respect to the *local* space. Contributions to this global CMB velocity arise from the orbital motion of the Earth in the Solar system (this contribution is apparent in the CMB observational data and is actually removed in the analysis), the orbital motion of the Solar system within the Milky Way galaxy, giving a speed of some 230 km/s giving together with local motion of the Solar system in the Milky Way, a net speed of some 250 km/s, and contributions from the motion of the Milky Way within the local cluster, and so on to perhaps larger clusters.

On the other hand the AM velocity is a vector sum of this *global* velocity and the net velocity associated with the *local* gravitational in-flows into the Milky Way and into the local cluster. This is because the observation of the CMB velocity does not pick up the local gravitational in-flows. Only gravitational lensing could affect that result, and that is an extremely small effect within the Milky Way. If the CMB velocity had been identical to the AM velocity then the in-flow interpretation of gravity would have been proven wrong. We therefore have three pieces of experimental evidence for this interpretation (i) the refractive index anomaly discussed previously in connection with the Miller data, (ii) the turbulence seen in all detections of absolute motion, and now (iii) that the AM velocity is different in both magnitude and direction from that of the CMB velocity.

That the AM and CMB velocities are different contributes to the explanation offered herein for the resolution of the 'dark matter' problem. Rather than the galactic velocity anomalies being caused by undiscovered 'dark matter' we see that the in-flow into non spherical galaxies, such as the spiral Milky Way, will be non-Newtonian. As well it will be interesting to determine, at least theoretically, the scale of turbulence expected in galactic systems, particularly as the magnitude of the turbulence seen in the AM velocity is somewhat larger than might be expected from the Sun in-flow alone. Any theory for the turbulence effect will certainly be checkable within the Solar system as the time scale of this is suitable for detailed observation.

3.10 Gravitational Waves

The velocity flow-field equation is expected to have solutions possessing turbulence, that is, fluctuations in both the magnitude and direction of the gravitational in-flow component of the velocity flow-field. Indeed all the gas-mode Michelson interferometer ex-
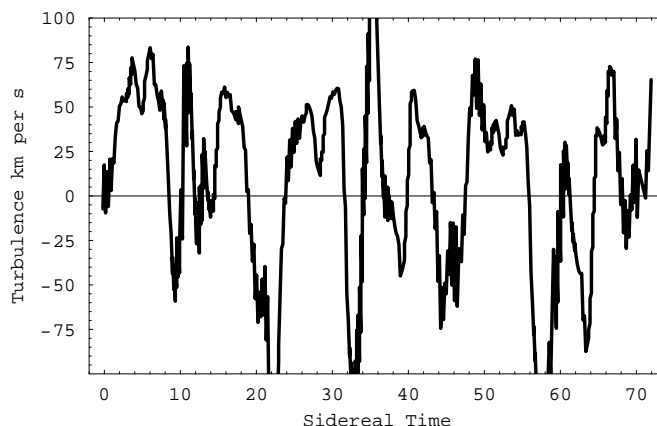
Figure 16: Speed fluctuations determined from figure 12 by subtracting a least squares best fit of the forms shown in figure 13b. A 1ns variation in travel time corresponds approximately to a speed variation of 27km/s. The larger speed fluctuations actually arise from a fluctuation in the cross-over time, that is, a fluctuation in the direction of the velocity. This plot implies that the velocity flow-field is turbulent. The scale of this turbulence is comparable to that evident in the Miller data, as shown in figure 7.

periments and coaxial cable experiments showed evidence of such turbulence. The first clear evidence was from the Miller experiment, as shown in figure 7. Miller offered no explanation for these fluctuations but in his analysis of that data he did running time averages. Miller may have in fact have simply interpreted these fluctuations as purely instrumental effects. While some of these fluctuations may be partially caused by weather related temperature and pressure variations, the bulk of the fluctuations appear to be larger than expected from that cause alone. Even the original Michelson-Morley data in figure 6 shows variations in the velocity field and supports this interpretation. However it is significant that the non-interferometer DeWitte data also shows evidence of turbulence in both the magnitude and direction of the velocity flow field, as shown in figure 16. Just as the DeWitte data agrees with the Miller data for speeds and directions the magnitude fluctuations, shown in figure 16, are very similar in absolute magnitude to, for example, the speed turbulence shown in figure 7.

It therefore becomes clear that there is strong evidence for these fluctuations being evidence of physical turbulence in the flow field. The magnitude of this turbulence appears to be somewhat larger than that which would be caused by the in-flow of quantum foam towards the Sun, and indeed following on from section 3.9 some of this turbulence may be associated with galactic in-flow into the Milky Way. This in-flow turbulence is a form of gravitational wave and the ability of gas-mode Michelson interferometers to detect absolute motion means that experimental evidence of such a wave phenomena has been available for a considerable period of time.

4 Conclusions

Here extensive experimental evidence has been presented for the existence of a quantum-foam substratum to space. Effects of motion through this substratum as well as flows related to gravity are evident in this experimental data. The evidence suggests that in fact the special relativity effects, which are well established by experiment, are being caused by absolute motion of systems through this quantum foam that is space. This amounts to an experimental confirmation of the Lorentzian interpretation of such relativistic effects. As well a new theory of gravity has been proposed based on a generalisation of both the Newtonian and General Relativity theories of gravity. It passes all the key existing tests, and as well also appears to be capable of explaining numerous gravitational anomalies. The phenomena present in these anomalies provide opportunities for further tests of the new gravitational physics. The experimental data also supports the conjecture herein that the gravitational flow displays turbulence. This amounts to the discovery of a form of gravitational wave. The new theory of gravity suggests that Newtonian gravity is only strictly applicable to cases of high spherical symmetry, such as the case of the Solar system which is dominated by the massive central star. In the case of a highly non-spherical spiral galaxy the new theory predicts gravitational forces very different from those predicted by the Newtonian theory. The use of the Newtonian theory in such cases has been used to argue for the existence of 'dark matter'. The new theory of gravity does away with the need for this concept of 'dark matter', which would also be consistent with the fact that after extensive searches no such 'dark matter' has been detected. Because General Relativity was constructed to agree with Newtonian gravity in the limit of low masses and low speeds, the apparent failure of the Newtonian theory in these cases casts serious doubt on the validity of the General Relativity formalism itself.

5 References

References

[1] Cahill R T 2002 *Process Physics: Inertia, Gravity and the Quantum, Gen. Rel. and Grav.* **34**, 1637-1656

[2] Cahill R T and Klinger C M 2000 *Self-Referential Noise and the Synthesis of Three-Dimensional Space, Gen. Rel. and Grav.* **32**(3), 529

[3] Cahill R T and Klinger C M 2000 *Self-Referential Noise as a Fundamental Aspect of Reality*, Proc. 2nd Int. Conf. on Unsolved Problems of Noise and Fluctuations (UPoN'99), Eds. D. Abbott and L. Kish, Adelaide, Australia, 11-15th July 1999, **Vol. 511,** p. 43 (American Institute of Physics, New York)

[4] Cahill R T, Klinger C M and Kitto K 2000 *Process Physics: Modelling Reality as Self-Organising Information, The Physicist* **37**(6), 191

[5] Cahill R T and Kitto K 2003 *Michelson-Morley Experiments Revisited and the Cosmic Background Radiation Preferred Frame, Apeiron* **10**, No.2. 104-117

[6] Chown, M 2000 *Random Reality, New Scientist*, Feb 26, **165**, No 2227, 24-2

[7] Michelson A A and Morley E W 1887 *Philos. Mag.* S.5, **24**, No. 151, 449-463

[8] Miller D C 1933 *Rev. Mod. Phys.* **5**, 203-242

[9] Illingworth K K 1927 *Phys. Rev.* **30**, 692-696

[10] Jaseja T S, Javan A, Murray J and Townes C H 1964 *Test of Special Relativity or Isotropy of Space by Use of Infrared Masers, Phys. Rev.* **A 133**, 1221

[11] Michelson, A.A. 1981 *Amer. J. Sci.* **S. 3 22**, 120-129

[12] Torr D G and Kolen P 1984 *Precision Measurements and Fundamental Constants*, B.N. Taylor and W.D. Phillips, Eds. *Natl. Bur. Stand.(U.S.), Spec. Publ.* 617, 675

[13] DeWitte R http://www.ping.be/~pin30390/

[14] Joos G 1930 *Ann. d. Physik* [5], **7**, 385

[15] Kennedy H P and Thorndike E M 1932 *Phys. Rev.* **42** 400-418

[16] Brillet A and Hall J L 1979 *Phys. Rev. Lett.* **42**, No.9, 549-552

[17] Braxmaier C, Müller H, Pradl O, Mlynek J, Peters A and Schiller S 2002 *Phys. Rev. Lett.* **88**, 010401

[18] Lipa J A, Nissen J A, Wang S, Striker D A and Avaloff D 2003 *Phys. Rev. Lett.* **90**, 060403-1

[19] Lineweaver C et al. 1996 *Astrophysics J.* **470**, 38

[20] Ives H 1939 *J. Opt. Soc. Am.* **29**, 183(1939); **38**, 413

[21] Kirkwood R L 1953 *The Physical Basis of Gravitation, Phys. Rev.* **92**(6), 1557

[22] Kirkwood R L 1954 *Gravitational Field Equations, Phys. Rev.* **95**(4), 1051

[23] Panlevé P 1921 *C. R. Acad. Sci.*, **173**, 677

[24] Gullstrand A 1922 *Ark. Mat. Astron. Fys.*, **16**, 1

[25] Hicks W M 1902 *Phil. Mag*, [**6**], 3, 256, 555; 9, 555

[26] Schwarz J P, Robertson D S, Niebauer T M and Faller J E 1998 *Science* **282**, 2230

[27] Munéra H A 1998 *Aperion* **5**, No.1-2, 37-54